Site-Specific PSHA: Combined Effects of Single-Station-Sigma, Host-to-Target Adjustments and Nonlinear Behavior. A case study at Euroseistest

Claudia Aristizabal, Pierre-Yves Bard, Céline Beauval

Site-Specific PSHA: Combined Effects of Single-Station-Sigma, Host-to-Target Adjustments and Nonlinear Behavior. A case study at Euroseistest

Claudia Aristizabal[1,2], Pierre-Yves Bard[1], Céline Beauval[1]

[1] Univ. Grenoble Alpes, CNRS, IRD, IFSTTAR, ISTerre, 38000 Grenoble, France.

[2] Suramericana S.A., Medellín, Colombia.

CA, ; P-YB., 0000-0002-3018-1047 ; CB, 0000-0002-2614-7268.

Ital. J. Geosci., Vol. 141, No. 1 (2022), pp. 5-34, 16 Figs ., 7 tabs.
https://doi.org/10.3301/IJG.2022.02

Research article

Corresponding author e-mail:
pierre-yves.bard@univ-grenoble-alpes.fr

Citation: Aristizabal C., Bard P-Y. & Beauval C. (2022) - Site-Specific PSHA: Combined Effects of Single-Station-Sigma, Host-to-Target Adjustments and Nonlinear Behavior. A case study at Euroseistest. Ital J. Geosci, 141 (1), 5-34, https://doi.org/10.3301/IJG.2022.02

Associate Editor: Claudio Chiarabba
Guest Editor: Giuseppe di Giulio

Submitted: 06 June 2021
Accepted: 01 November 2021
Published online: xx February 2022

ABSTRACT

This study takes advantage of the available information for an example, well-known, site in Greece (TST site at Euroseistest) to illustrate the epistemic variability in probabilistic seismic hazard assessment (PSHA) estimates. The purpose is not to perform an exhaustive site-specific PSHA at this particular site, but to investigate the sensitivity of the results to the approach used for including site effects, from basic ones to more demanding and realistic ones, in order to better appreciate the "benefits" versus the required costs and efforts of each approach. The TST site, located at the center of the Mygdonian basin in North-Eastern Greece is characterised by soft shallow soils over thick, medium stiffness deposits with a complex underground geometry, resting on very hard bedrock. Three different levels are considered for the incorporation of site response, from level 0 (generic or partially generic) to site-specific ones, with linear (level 1) or non-linear (level2) site response analysis. The basic methods rely on one or several site proxies (V_{S30}, V_{SZ} and f_0), whereas the most complex ones couple site response assessment (instrumental or numerical, implying site-specific characterization or instrumentation) with various reference rock hazard adjustments (single-station sigma, host-to-target adjustments, depth correction). Results are compared in terms of Uniform Hazard Spectra for a 5000 years return period, a typical value for critical facilities. For each level, the epistemic uncertainties are described and their impacts on hazard estimates are quantified. The use of the V_{S30} proxy in ground-motion prediction equations (GMPEs) leads to a clear underestimation of the hazard for the linear case (i.e., short return periods), especially around the site fundamental period, because of resonance and basin effects. On the other hand, soil nonlinearity largely impacts the hazard estimates, and linear amplification approach leads to an overestimation of the hazard, with unrealistic high levels at very long return periods. Site-specific hazard estimates for thick, Euroseistest-like sites, with complex geometry and rheology, are thus shown to come up against several additional epistemic uncertainties implying a large approach-to-approach variability. This may lead to increased hazard estimates, counterbalancing the decrease due to the use of reduced, single-site aleatory uncertainty in reference rock hazard estimates. For the time being, it thus looks unrealistic to promise a systematic reduction in hazard estimates with site-specific studies, while it might also indicate that uncertainties in generic hazard estimates could presently be underestimated.

KEY-WORDS: Site Effects, Epistemic Uncertainty, PSHA, Single-station-sigma, Host-to-target adjustments, Linear and Nonlinear behavior, Site Response analysis.

INTRODUCTION

Several recent dramatic events drew the attention on the need to carefully reassess the very rare, high-impact, seismic hazard for large urban centers and critical facilities. Presently, the trend all over the world is to more and more rely on probabilistic approaches to estimate seismic hazard, aiming at determining ground-motion exceedance probabilities over future time windows. Past examples have shown that site effects can significantly amplify ground motions (e.g., in Mexico City during the 1985 Michoacán and 2017 Puebla earthquakes, see Sánchez-Sesma,1998; Chávez-García & Bard, 1994; Çelebi et al., 2018; Galvis et al., 2018. Several authors have thus been working on the development of methods to estimate hazard curves and

uniform hazard spectra (UHS) including site effects within a probabilistic framework (Kramer, 1996; Lee et al., 1998, 1999; Lee, 2000; Tsai 2000; Silva et al., 2000; Cramer, 2003; Bazzurro & Cornell, 2004a,b; Stewart et al., 2006; Papaspiliou et al., 2012a,b; Rathje et al., 2015; Barani & Spallarossa 2016, Haji-Soltani & Pezeshk, 2017; Aristizabal et al., 2018b).

Despite the clear evidence of the site effects impact on ground estimates and its variability, most probabilistic seismic hazard studies are still focused on rock sites (McGuire & Toro, 2008). The amplification of the site is often added later by applying amplification factors. This crude way of integrating site effects may lead to hazard estimates that are potentially either under-estimated (e.g., at some frequencies when resonance effects are ignored) or over-estimated (e.g., when nonlinear effects are not properly accounted for). As an example, the site amplification factors accounted for in the present version of Eurocode 8 for different site classes, are the same whatever the considered location in Italy, Greece, or any other active seismic area, therefore somehow ignoring the non-linearity of site response. Similarly, many ground-motion prediction equations (GMPEs) still in use in PSHA codes do not account for nonlinear behaviour. Nonetheless, among the newest (e.g., NGAW2, Bozorgnia et al., 2014; RESORCE, Douglas et al., 2014) several models account for the soil nonlinearity as a function of the acceleration level. Besides non-linearity, other factors may lead to significant variability in site-specific hazard estimates, depending on the geometry of the site (surface and underground topography potentially leading to 2D or 3D effects), the hardness of the local bedrock, and the approach used for the estimation of site amplification (instrumental or numerical).

The purpose of the present study is to illustrate the epistemic variability in site-specific PSHA estimates on one example site, the well-studied Euroseistest site in Greece. All hazard calculations are based on the area source model from SHARE (Woessner et al., 2015). After a quick methodological overview and a presentation of the study area, an overview of the various prerequisites needed for PSHA is given, depending on the approach and the characteristics of reference rock. The results obtained with the different approaches are then presented first for the reference rock and then at the site surface. Their comparison leads to in-depth discussions emphasizing the epistemic uncertainties related to each approach and their impact on hazard estimates. At last, recommendations are provided on how to integrate site effects into PSHA; while most complex approaches intend to better model the physics of site response, they are generally associated with an additional level of epistemic uncertainty.

METHODOLOGICAL OVERVIEW

Following Cramer (2003), Bazzurro & Cornell (2004b), Rathje et al. (2015) and Pecker et al. (2017), the incorporation of site effects in PSHA analyses may be performed either with hybrid methods where the probabilistic rock hazard is combined with a deterministic site response, or with fully probabilistic methods where both the rock hazard and the site response are considered in a probabilistic framework. Besides, the site response may be accounted for either in a crude way (using a gross proxy) or through more elaborated site-specific methods. This fourfold general classification based on these two criteria may be further refined according to the approach selected for the estimation of site amplification and depending on the adjustments that may be required for the rock hazard. Table 1 proposes a detailed classification for the range of methods that include site effects into PSHA, with increasing level of complexity: level 0 corresponds to basic generic approaches, level 1 corresponds to linear site-specific responses in hybrid methods – for which hybrid and fully probabilistic approaches provide the same results -, and finally level 2 accounts for non-linear site response with hybrid of fully probabilistic approaches.

Furthermore, Level 1 is broken down into 3 alternative methods, depending on the way the amplification function is estimated. Level 2 is broken down into 5 alternative methods, with different levels of complexity; only 2 out these 5 methods are applied in the present study. The horizontal lines in Table 1 correspond to issues that may be common to different approaches and require specific actions. For instance, non-standard reference rock conditions (hard rock, reference site at depth) call for specific hazard adjustments, while site-specific amplification allow to reduce the ground-motion variability to be considered in the GMPE for the rock PSHA estimates.

The aim of the present study is to apply these different approaches to the Euroseistest site, and each of the specific items in these linesand columns will be commented in more detail in the following on the Euroseistest example.

STUDY AREA: LOCATION, RECORDINGS AND UNDERGROUND STRUCTURE

The Euroseistest site is located at the center of the Mygdonian sedimentary basin at about 30km to the North East of Thessaloniki in northern Greece (Figure 1a). The Mygdonian basin has been extensively investigated within the framework of various European projects (Euroseistest, Euroseismod, Euroseisrisk, Ismod) and recently in an extensive benchmarking exercise on the numerical simulation of ground-motions (Maufroy et al., 2015, 2016, 2017). The basin is densely instrumented with surface accelerometers, as well as a vertical array with 6 sensors over 200 m depth at the central station of the basin TST. Stations are jointly maintained by ITSAK and AUTH. The accelerometric recordings have been gathered and made available in a specific open access database (Pitilakis et al., 2013). The stations considered in the present study are located at the center of the Euroseistest basin, one at the surface, TST_0, and the other one at the bottom of the basin, TST_{196}, at 196 m depth (Figure 1b).

Instrumental Characterization

This instrumental database has given rise to numerous investigations aiming at characterizing the site amplification with respect to the various possible reference rocks. The site amplification estimates may be found in Riepl et al., 1998; Raptakis et al., 1998; Ktenidou et al., 2015a; 2018 and Maufroy et al., 2017. These instrumental estimates depend on the used dataset, and also on the selected reference sensor (surface or downhole). The reference stations considered in the present study are either the PRO station, outcropping on

Table 1 - Generic, partially Site-Specific and Site-Specific Approaches for the integration of site effects into Probabilistic Seismic Hazard Assessment.

		Level 0 Generic or Partially Site-Specific Approaches		Site-Specific Approaches							
				Level 1 Linear Site Response AF(f) Ground-motion-independent			Level 2 Nonlinear Site Response AF (Sa, f) Ground-motion-dependent				
		Level 0a	Level 0b	Level 1a	Level 1b	Level 1c	Level 2a	Level 2b	Level 2c	Level 2d	Level 2e
Site Effects Estimation Method		Use of proxy in GMPEs. e.g. V_{S30}, measured or inferred, linear or non-linear.	Site effects by proxy in GMPEs and Amplification Factors. (e.g. SAPE (Vs,z , *fo*). Cadet et al., 2012a) Other proxies could also be included)	Instrumental	*Instrumental*	Numerical	Mostly numerical, instrumental only if hundreds of recordings available at the site, spanning a wide enough level range				
				Hybrid Method Based on disaggregation Cramer 2003 UHS Rock • AF(*f*)			Hybrid Method	Full Probabilistic Integration Based Method	Analytical approximation of the full convolution method	Classical PSHA with Site-Specific GMPE	Full Probabilistic Stochastic Method
				AF(*f*) from Site-specific Residual (δS2Ss) and φ_{ss} from GMPEs) (e.g. Ktenidou et al., 2015a, 2018)	AF(*f*) from Standard Spectral Ratios (SSR), with rock reference station outcropping or downhole (e.g. Raptakis et al., 1998)	AF(*f*) from Numerical simulations of weak ground-motion 1D, 2D or 3D (e.g. Aristizabal, 2018a;b)	AF(Sa,*f*) from numerical simulations of strong ground-motion 1D, 2D or 3D (e.g. Bazzurro & Cornell, 2004a)	Full PSHA Soil (Cramer 2003, Bazzurro & Cornell, 2004a,b; Rathje et al., 2015)	Classical PSHA Rock Hazard Curve *AF(Sa,*f*) (e.g. Bazzurro & Cornell, 2004a,b; Aristizabal et al., 2018a;b)	Classical PSHA Soil (e.g. Bazzurro & Cornell, 2004a,b; Papaspiliou et al., 2012a,b)	Stochastic PSHA Soil (e.g. Aristizabal et al., 2018a;b)
Prerequisite: Rock hazard		Not Necessary	Standard-rock V_{S30} = 800 m/s	No /Yes (Verify if included inside δS2Ss residuals)	Site-specific Bedrock (e.g. V_s = 2600 m/s)						
GMPEs Host-to-target Adjustment		No	No		Yes (If necessary)						
Uncertainty in GMPEs Rock Hazard		Total Standard Deviation (σ total)		σ total or σ_{ss}	Single-station Standard Deviation (σ_{ss})						
Site Response Uncertainties	Aleatory	φ - No Additional Uncertainty		$\varphi_{SS,S}$ or φ_{SS} if available, No Additional Uncertainty							
	Epistemic	n/a	Various SAPE (*f*)	Uncertainty on δS2Ss	Different AF (Instrumental or Numerical), Soil Profiles, Degradation Curves, Propagation Codes, 1D, 2D or 3D Models.						
Calculation of Soil Hazard				Classical PSHA	Approach 1 and 2 NUREG 6728		n/a	n/a	Approach 4 NUREG 6728	Approach 3 NUREG 6728	
		n/a	SAPE (*f*)	δS2Ss							

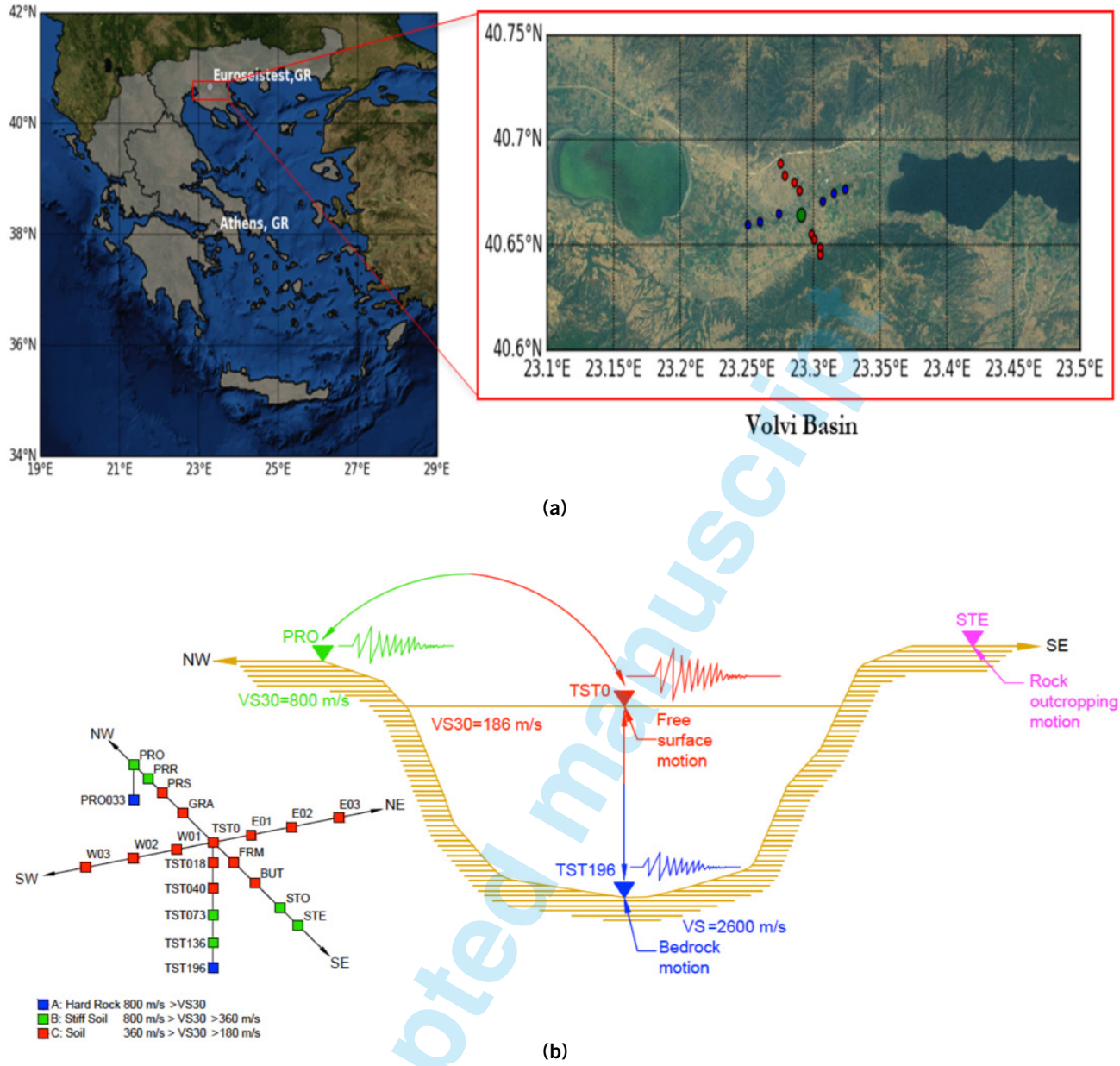

Fig. 1 - (a) Euroseistest location at Volvi basin in North Eastern Greece. (b) Euroseistest PRO-STE simplified cross-section with the main stations used in this study (TST_0 and TST_{196}), as well as the sketch of the current station array (modified from Pitilakis et al., 1999).

the valley edge, or the downhole TST_{196} station at the bottom of the basin (Figure 1b). We use the amplification estimates by Raptakis et al. (1998) and Ktenidou et al. (2015a), (2018). Besides, for the downhole sensor TST_{196} station, located on hard rock, an analysis of the "κ" parameter characterizing the high-frequency decay is required. We use the values from Ktenidou et al., (2015b).

Underground structure

To perform a site-specific hazard assessment at Euroseistest, the geological, geophysical and geotechnical data at the site of interest are needed. Previous studies at Euroseistest provide a detailed soil profile, the geometry of the basin, the shear-wave velocity at both the bedrock and at the surface, which allow to properly parameterise the soil properties. Given the uncertainties in such measurements, different velocity models have been proposed for the Euroseistest basin (e.g., Jongmans et al., 1998, Raptakis et al., 2000, Chávez-García 2000). For the present study, they have been condensed in a relatively simple profile consisting of a stack of horizontal layers (Figure 2a) associated with simplified degradation curves (Figure 2b) taken from Pitilakis et al. (1999). As shown in the shear-wave velocity profile (Figure 2a), the Euroseistest basin is described by a soft-soil at the top of the basin (Figure 2a), with an average shear wave velocity on the first 30 m of Vs_{30}=186 m/s. At the bottom of the basin, a large impedance contrast between sediments and bedrock is identified, since the bedrock has a shear wave velocity of 2600 m/s at 196 m depth.

The different parameters required in the present study to model the soil profile are displayed in Table 2: Vs, shear wave velocity;

Vp, compressive wave velocity; ρ, material density; Q_S, anelastic attenuation factor; φ: friction angle; K_0: coefficient of lateral earth pressure at-rest. Instrumental and numerical studies performed have shown a fundamental frequency (f_0) around 0.6 - 0.7 Hz (Riepl et al., 1998, Raptakis et al., 2000, Maufroy et al., 2015, 2016 and 2017).

PREREQUISITES FOR SITE-SPECIFIC APPROACHES

If the reference rock considered in the site amplification is much harder than standard rock (e.g., if TST_{196} is considered), as the GMPEs currently used in PSHA are valid only for standard rock (~800 m/s), corrections must be applied to the UHS obtained to adapt it to hard rock conditions. Moreover, when site-specific approaches are considered, the variability (sigma) of the GMPE used to estimate probabilistic rock hazard may be reduced (Al Atik et al., 2010).

Reference-rock issues

At Euroseistest, the reference rock used to estimate site amplification AF(f) is located either at depth (sensor TST_{196}, Figure 1b) or on an outcrop (sensors STE or PRO, Figure 1b). The TST_{196} location corresponds to a S-wave velocity of 2600 m/s (Table 2) which is much higher than the standard rock velocity around 800 m/s considered for rock condition in current GMPEs. If TST_{196} has been used to estimate the site amplification function, then the uniform hazard spectrum at 2600 m/s is required. The uniform hazard spectrum obtained for 800m/s with a GMPE must be modified using correction factors accounting for (1) a higher shear wave velocity, (2) different regional and local attenuation characterised through the high frequency attenuation factor, κ, (Anderson & Hough, 1984); and (3) the effects of constructive and destructive interferences between upgoing and down-going waves, which are different at surface and depth (Cadet et al., 2012).

Rock to Hard-rock corrections and implementation for TST_{196}

There are actually very few GMPEs derived for hard-rock (e.g., Laurendeau et al., 2018), and the shear wave velocity validity range of most GMPEs does not exceed 1200-1500 m/s, due to lack of data on hard rock sites. In addition, it is generally accepted that

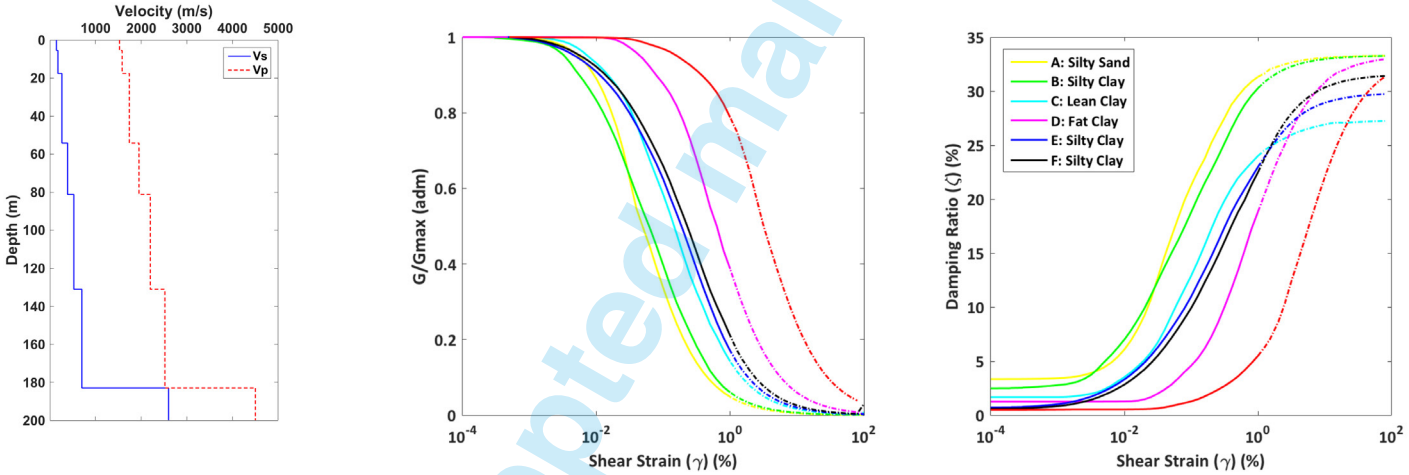

Fig. 2 - Euroseistest case study: (a) 1D shear wave, Vs, and compressive wave, Vp, soil profiles between TST_0 and TST_{196} stations (see Figure 1b) based on Raptakis et al.,1998; (b) non-linear degradation curves showing the decrease of the shear modulus with shear strain, and (c) the increase of shear damping with shear strain (Pitilakis et al., 1999).

Table 2 - Material properties of the Euroseistest soil profile (based on Raptakis et al., 1998).

Layer	Depth (m)	Vs (m/s)	Vp (m/s)	ρ (kg/m³)	Q_S	ϕ	K_0
1	0.0	144	1524	2077	14.4	47	0.26
2	5.5	177	1583	2083	17.7	19	0.67
3	17.6	264	1741	2097	26.4	19	0.68
4	54.2	388	1952	2117	38.8	27	0.54
5	81.2	526	2200	2151	52.6	42	0.33
6	131.1	701	2520	2215	70.1	69	0.07
7	183.0	2600	4500	2446	-	-	-

*Water Table at 1 m depth. Vs: shear wave velocity. Vp: Compressive wave velocity. ρ: soil density. Q_S: Anelastic attenuation factor. ϕ: Friction angle. K_0: Coefficient of earth pressure at rest.

harder rocks are associated to smaller attenuation, which may affect significantly the high-frequency contents.

Several approaches have thus been proposed to adjust the ground motion predicted for standard rock to hard rock (e.g., Campbell, 2003; Al Atik et al., 2014; Laurendeau et al., 2018), generally referred to as "host-to-target adjustment" (HTTA) procedures. Their goal is to take into account any possible difference in source, propagation, and rock site conditions between the so-called host area with many strong motion data where GMPE can be developed (e.g., Western North America, or the Mediterranean area, or Japan), and the target site, using physics-based models such as the stochastic model presented in detail in Boore (2003). Detailed descriptions and critical discussions of pros and cons of each HTTA approach can be found in Bard et al. (2020). HTTA procedures most often combine shear wave velocity corrections (VSC) and high frequency attenuation correction or kappa corrections (KC). The target site here is the Euroseistest TST station at 196m depth.

- Shear wave velocity correction (impedance correction)

The TST_{196} reference station is located on very hard rock at the bottom of the basin, with a shear wave velocity of 2600 m/s. The shear wave correction (VSC) is performed following the approach developed by Boore (2003) based on stochastic modeling of ground motion. A "crustal amplification function" A(f) must be derived, directly linked to the crustal velocity profile Vs(z) between the source depth and the surface. This amplification function ignores resonance phenomena and accounts only for the impedance ratio between the source at depth and the surface. The frequency dependence is established through the quarter wavelength approximation: for a given frequency f, the impedance to be considered is the average one down to a depth corresponding to a quarter wavelength. The velocity correction VSC(f) is the ratio between the crustal amplification function associated to the velocity profile of the actual site (here V_S = 2600 m/s) and the crustal amplification function associated to a standard rock site with V_{S30} = 800 m/s:

$$VSC(f) = \frac{A(f(z))_{Vs=2600m/s}}{A(f(z))_{Vs30=800m/s}} \quad \text{Eq. 1}$$

In practice, since the deep velocity profile is only rarely known, crustal amplification functions are often estimated on the basis of a family of "generic profiles" VS(z, V_{S30}) which have a common velocity at large depth (3600 m/s beyond 8 km depth) and are parameterised according to the shallow velocity V_{S30} (Boore & Joyner, 1967; Cotton et al., 2006). Figure 3a displays the amplification functions determined for the standard rock and the hard-rock sites, while Figure 3b shows the VSC correction obtained applying Eq. 1. This velocity correction factor must be applied directly to the Fourier spectrum corresponding to standard rock UHS. For further information on how to derive the crustal amplification functions the reader should refer to Boore (2003).

- High Frequency Attenuation Factor Correction (κ correction or KC):

Anderson & Hough (1984) proposed that the shape of the Fourier acceleration spectrum at high frequencies could be generally described in Eq. 2.

$$A(f) = A_0 e^{-\pi f \kappa} \quad \text{Eq. 2}$$

Where A_0 is a constant that depends on source properties, epicentral distance, and other second order factors, *f* is the frequency and κ is the high-frequency attenuation factor or the spectral decay parameter of the Fourier amplitude spectrum. The value of κ describes the systematic behavior of the spectral decay of S waves, related to the attenuation of such waves when propagating through the crust (regional attenuation) and when propagating upward just under the recording site. It is generally considered as the sum of terms, $\kappa = \kappa_0 + m\,R$, where the linear increase with epicentral (or hypocentral) distance R is related to the regional characteristics of S-wave damping (at large crustal depth), while κ_0 is a site-specific term corresponding to the damping profile just under the site.

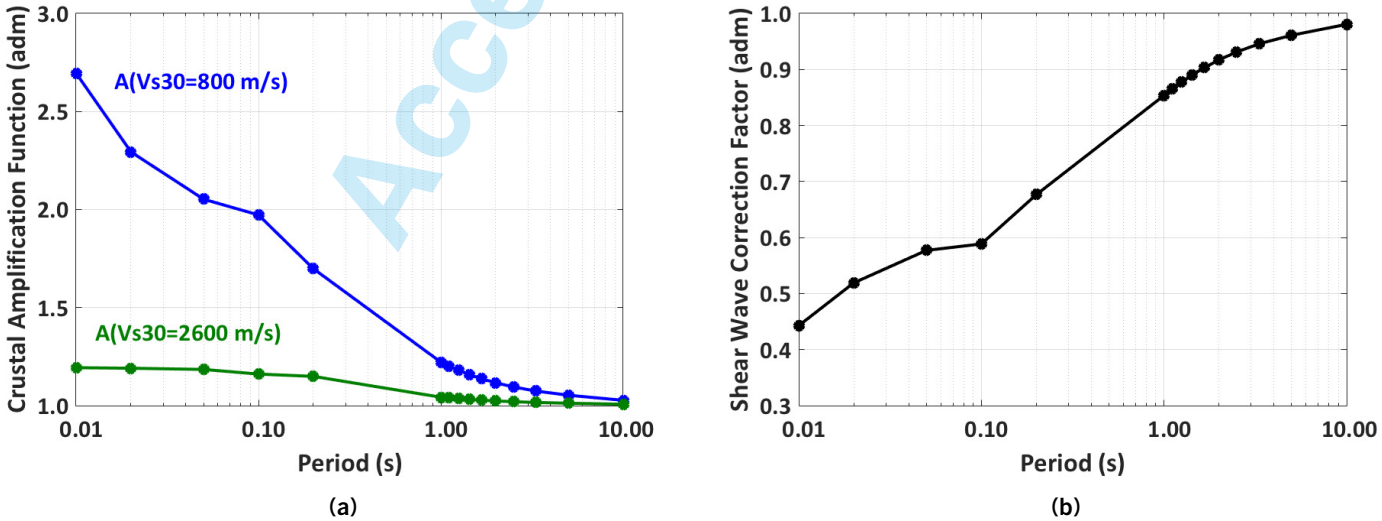

Fig. 3 - Rock to hard rock corrections for TST site at Euroseistest. (a) Crustal amplification functions for a standard rock site (V_S=800 m/s, blue) and for a hard-rock site (V_S=2,600 m/s, green). (b) The Shear Wave Velocity Correction (VSC) corresponding to the ratio between these two quarter-wavelength crustal amplification functions.

Returning to HTTA, the host region and the target site may have different shear attenuation and therefore different κ values. The distance dependent term is most often accounted for through the spatial decay coefficients and is often thought not to vary much between regions with a similar tectonic background. On the contrary, the site-specific term κ_0 is expected to vary strongly, and a high-frequency attenuation factor correction (KC) is often implemented in HTTA procedures. Currently, several methodologies describing how to account for κ_0 effects are available in the literature (Campbell, 2003; Cotton et al., 2006; Douglas et al., 2006; Van Houtte et al., 2011; Bora et al. 2013). The κ_0 correction performed here follows the methodology proposed by Al Atik et al. (2014), which is the most recent and quite widely used.

In principle, κ_0 should be known for both the host GMPE and the target site. In general, κ_0 is known for the target but not for the host. The host site is characterised by many recordings from different (rock and soft soil) sites without any special consideration for their high frequency decay. Therefore, this κ_0 correction (KC) may vary from one GMPE to another, as the average host κ_0 may vary from one strong-motion data base to another. The κ correction is therefore more complex than the VSC correction, the κ -scaling factors must be determined for each GMPE.

We follow the main steps of Al Atik et al. (2014) technique to generate κ_0 correction factors for UHS scaling at Euroseistest:

- Use the GMPE to predict the host response spectrum (RS) for a site with V_{S30}=800 m/s. The response spectrum is determined for a scenario earthquake deduced from disaggregation at the Euroseistest site. Our disaggregation calculations show that the magnitude range contributing the most to the hazard at 5000 years return period is Mw=[5.5-7.5], with the maximum of contributions around Mw 6.5, at distances up to 20 km (PGA and 0.2 second spectral period). Therefore, we generate a host response spectrum for a magnitude 6.5 at 10 km (RS_{800}).
- Calculate a Fourier amplitude spectrum (FAS_{800}) consistent with this response spectrum, RS_{800}, using inverse random vibration theory (IRVT) as implemented in the program Strata (Kottke & Rathje, 2008a, b).
- Multiply the host FAS_{800} by the Vs correction factors to obtain the Fourier amplitude spectrum of a rock with a Vs=2600 m/s, $FAS_{2600.}$
- Estimate κ_h from the FAS_{2600} based on the slope in the high frequency spectrum by fitting the Anderson & Hough (1984) κ function (see Eq. 2).
- Apply κ scaling by multiplying the host FAS_{2600} by the following factor: (see Eq. 3).

$$e^{(-\pi f (\kappa_t - \kappa_h))} \quad \text{Eq. 3}$$

- Convert κ-scaled FAS to response spectrum using random vibration theory, to obtain RS_{2600}.
- Calculate the V_S-κ scaling factor for response spectrum by dividing the κ-scaled response spectrum (RS_{2600}) by the response spectrum at V_{S30}=800 m/s (RS_{800})
- Apply this scenario-specific correction factor to the UHS obtained at 800 m/s, to get the UHS at 2600 m/s.

For the study to be fully complete, uncertainties on the target and host kappa values should be tracked and quantified in order to estimate a median V_S-κ scaling factor with associated uncertainties for each GMPE. In the present example, for sake of simplicity, only single values were considered for κ_h and κ_t. The target κ_t value was estimated as κ_t = 0.024 s from Ktenidou et al. (2014), (2015b). The host kappa values have been estimated according to the above procedure (items 1 to 4) for different GMPEs. The results listed in Table 3 exhibit a significant variability in host-kappa values from one GMPE to another. These values are consistent with those found by Kottke 2017.

- Combined Vs- κ Correction (VSC-KC):

Most often *Vs* and κ scaling must be both performed. As shown in the previous section, we apply κ correction after the *Vs* correction in order to avoid a bias on the final target kappa value. The decision of whether to apply first the V_S correction and then the κ correction or vice versa is not straightforward. We do not follow Al Atik et al. (2014) who propose to start with the κ correction.

The Vs-κ correction is obtained as the ratio between the VSC-KC corrected hard-rock response spectrum (Figure 4a; red) for a given scenario (here Mw=6.0 and Rhyp=10 km), and the response spectrum on standard rock predicted by the GMPE for the same scenario (Figure 4a; blue). The ratio in Figure 4b displays two main features: (1) a deamplification effect over the whole spectral period range, varying between 0.75 and 0.95, linked to the higher shear-wave velocity with respect to standard rock, (2) a short-period modulation of this deamplification [0.02-0.1 s] linked to the smaller kappa value, decreasing from κ_h = 0.0395 s for the Akkar et al. (2014 GMPE), to κ_t = 0.0024 s at the Euroseistest.

Depth Correction Factor (DCF)

The uniform hazard spectrum obtained with current GMPEs corresponds to a site at the surface. If the reference used for estimating the site amplification is located at depth, a depth correction is required to move the UHS from the surface to depth. In the present case, we applied the procedure proposed by Cadet et al., 2012a to account for the depth dependence of interferences between up-going and down-going waves. At the surface

Table 3 - Host kappa, κ_h, for different GMPEs and the considered scenario (Mw=6.5, R=10 km)

GMPE	Akkar & Bommer 2010 (AB10)	Cauzzi & Faccioli 2008 (CY08)	Zhao et al., 2006 (ZA06)	Akkar et al. 2014 (AA14)	Cauzzi et al. 2014 (CA14)	Boore et al., 2014 (BA14)	Chiou & Youngs 2008 (CY14)
Kappa Host (k_h)	0.0366	0.0331	0.0353	0.0395	0.0312	0.0442	0.0321

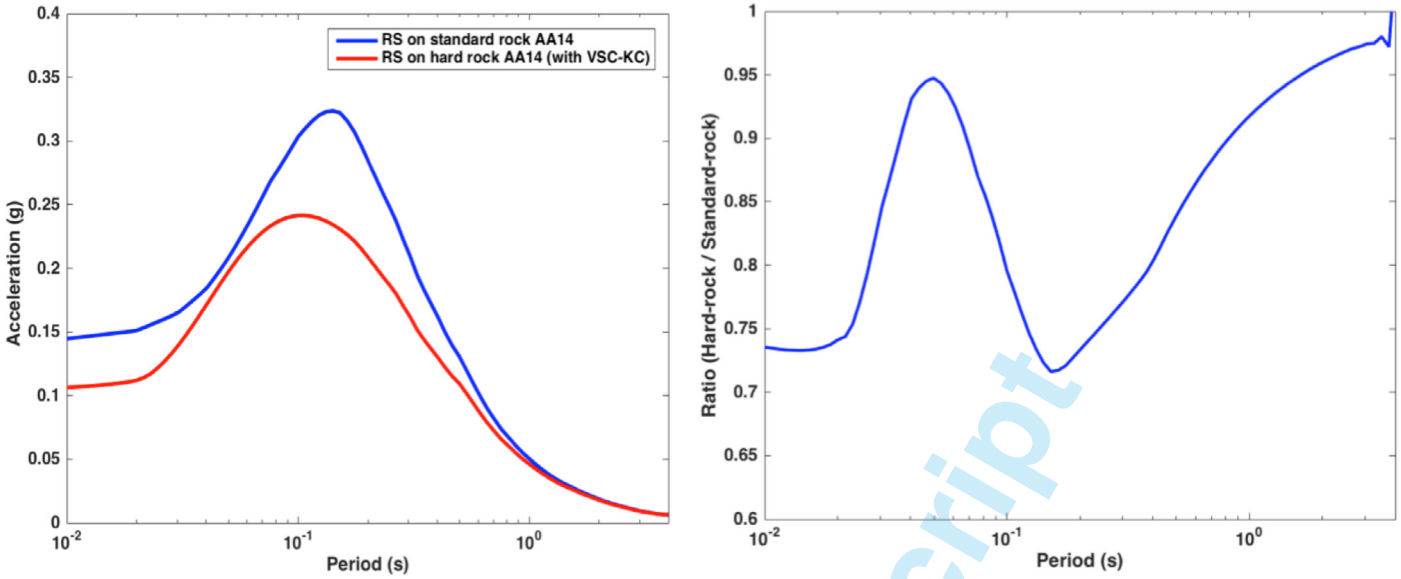

(a) (b)

Fig. 4 - Combined Vs-κ correction at Euroseistest site: (a), response spectrum (RS) on standard rock predicted by the GMPE (V_{S30} 800 m/s, blue) and Vs-κ corrected response spectrum (RS) (V_{S30}=2600 m/s, red); (b) Vs-κ scaling factor, which is the ratio between the scaled response spectrum (V_{S30}=2600 m/s) and the response spectrum predicted by the GMPE at V_{S30} =800 m/s. The GMPE used is Akkar et al., 2014. Calculations performed for a scenario earthquake Mw 6.0 at 10km. The target κ is 0.0024 s.

they systematically interfere constructively (free-surface effect), while at depth they may interfere destructively or constructively depending on the ratio between the depth and the wavelength. This depth correction factor (DCF) is described in the dimensionless frequency space as the product of two frequency-dependent functions, C1 and C2 (Eq. 4).

$$\mathrm{DCF} = \mathrm{C1(f)} \cdot \mathrm{C2(f)} \qquad \text{Eq. 4}$$

C1 (Eq. 5) is linked to the free surface and attenuation effects, while C2 (Eq. 6) is linked with the destructive interference effects mainly around the fundamental frequency. C2 is therefore peaked at the fundamental destructive frequency f_{dest} and characterised by a peak amplitude A. The proposed functional forms are a smoothed step (arctan) for C1, and Gaussian like for C2 (see Cadet et al., 2012a for more details):

$$C1(f) = 1 + \frac{B \cdot \arctan\left(f/f_{dest}\right)}{\pi/2} \qquad \text{Eq. 5}$$

$$C2(f) = 1 + (A-1) \cdot e^{\frac{-(f/f_{dest}-1)^2}{(2\sigma)^2}} \qquad \text{Eq. 6}$$

Following Cadet et al. (2012a), we use the generic values for the correction of response spectra, i.e., A=1.8, σ=0.15, and B=0.8, while the frequency dependence is controlled by the actually measured destructive frequency of the soil column (f_{dest} = $\overline{Vs}$/4H = 0.7 Hz), where H is the depth of the downhole instrument and $\overline{Vs}$ the average velocity over that depth.

Purely instrumental correction: use of site-specific residual ($\delta_{S2S,\,rock}$)

As explained in Bard et al. (2020), the availability of numerous recordings at the rock reference sites allows to use a purely instrumental correction, derived from the systematic comparison of reference rock recordings with the GMPE predictions. Also, as described in Al Atik et al. (2010), the corresponding residuals Δ_{es} (Eq. 7) can be decomposed in a between-event term δB_e and a δW_{es} within-event term, where subscripts e and s stand for event e and station s:

$$\Delta_{es} = \delta W_{es} + \delta B_e \qquad \text{Eq. 7}$$

Then, the within-event residual term, $\delta W_{es,}$ can be further broken down into a site term, $\delta S2S_s$, and a site-and-event corrected residual δWS_{es} with zero mean, as follows:

$$\delta W_{es} = \delta S2S_s + \delta WS_{es} \qquad \text{Eq. 8}$$

Ktenidou et al. (2015a) performed this analysis and calculated $\delta S2S_s$ term at TST site using the Akkar et al. (2014) GMPE, for various oscillator periods (Eq. 9 and Eq. 10). They obtained the values listed in Table 4, separately for the surface (TST_0) and downhole sites (TST_{196}). For each site, the $\delta S2S_s$ term has been calculated either applying the GMPE with its site term S based on the value of the V_{S30} proxy (WIST), or without its site term (WOST) with respect to standard rock reference (V_{S30} = 800 m/s).

$$ln(Y) = ln[Y_{REF}(Mw, R, SoF)] + ln[S(V_{S30}, PGA_{REF})] + \varepsilon\sigma \qquad \text{Eq. 9}$$

Nonlinear term

$$ln(S) = \begin{cases} b_1\, ln\left(\frac{V_{S30}}{V_{REF}}\right) + b_2\, ln\left[\frac{PGA_{REF} + c\left(\frac{V_{S30}}{V_{REF}}\right)^n}{(PGA_{REF} + c)\left(\frac{V_{S30}}{V_{REF}}\right)^n}\right] \\ b_1\, ln\left[\frac{min(V_{S30}, V_{CON})}{V_{REF}}\right] \end{cases} \quad \text{Eq. 10}$$

Linear term

The corresponding "site-specific" $\delta S2S_s$ terms based on residuals are plotted in Figure 6a as a function of oscillator period (red curves). Residuals at the downhole site are negative when calculated with respect to standard rock (WIST, red dashed curve). Moreover, residuals are larger in the WOST case (dashed lines) than in the WIST case (negative for TST_{196}, and positive for TST_0). At this stage, site-specific residuals (Figure 6a) and depth corrections (Figure 5) cannot be compared, since the DCF correction should be combined with the VSC-KC correction before being compared with the residual approach.

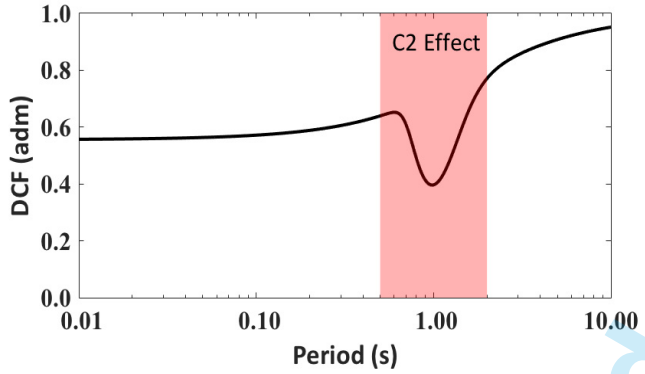

Fig. 5 - Depth correction factors (DCF) for response spectra at the Euroseistest derived from Cadet et al., 2012a.

GMPE aleatory variability to be considered for the rock hazard

In the case of the generic approach, if site effects are accounted for through a simple proxy (level 0 in Table 1), the rock hazard must be evaluated with the total variability predicted by the GMPE. However, the rock hazard (UHS_{rock}) may be estimated with a reduced variability when the site amplification is estimated specifically for the site under study (levels 1 and 2, Table 1 , site-specific approaches, Al Atik et al., 2010).

Breaking down sigma

Traditionally, empirically based ground-motion prediction equations have been built based on the ergodic assumption, (Anderson & Brune, 1999; Abrahamson 2012), meaning that the ground-motion variability evaluated from a database with multiple sites and source-to-site paths is applicable to describe ground-motion variability at another site. However, when the site amplification is well characterised, this ergodic standard deviation may be replaced by a "single-station" standard deviation (σ_{ss}) estimated using the site-specific residuals at the site (e.g., Rodriguez-Marek et al., 2011, 2013).

The total standard deviation of a GMPE (σ) is usually split into between-event (τ) and within-event (ϕ) variability (e.g. Al Atik et al., 2010):

$$\sigma = \sqrt{\phi^2 + \tau^2} \quad \text{Eq. 11}$$

Where σ, τ and ϕ are, respectively, the standard deviation of the Δ_e , δB_e and δW_{es} residuals (Eq. 7). The within-event variability ϕ^2 may be in turn considered as the sum of two components, ${\phi_{S2Ss}}^2$ and ${\phi_{ss}}^2$, where ϕ_{S2Ss} is the standard deviation of $\delta S2S_s$ and characterises the site-to-site variability of the mean site residuals, while ϕ_{ss} is the standard deviation of the within-event residual term (δW_{es}),

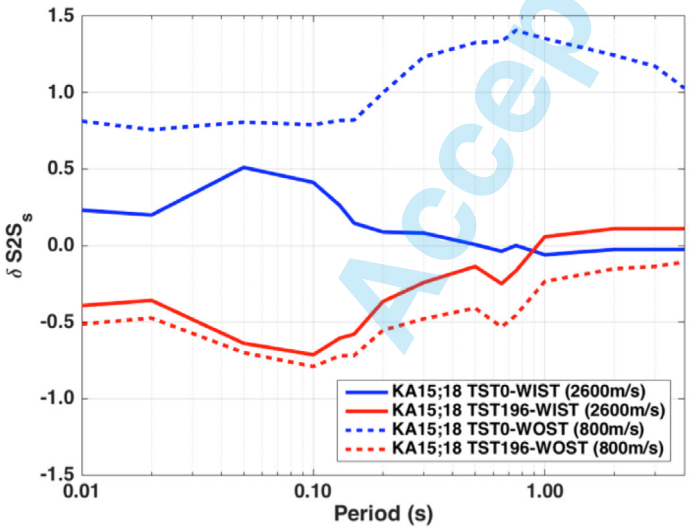

(a)

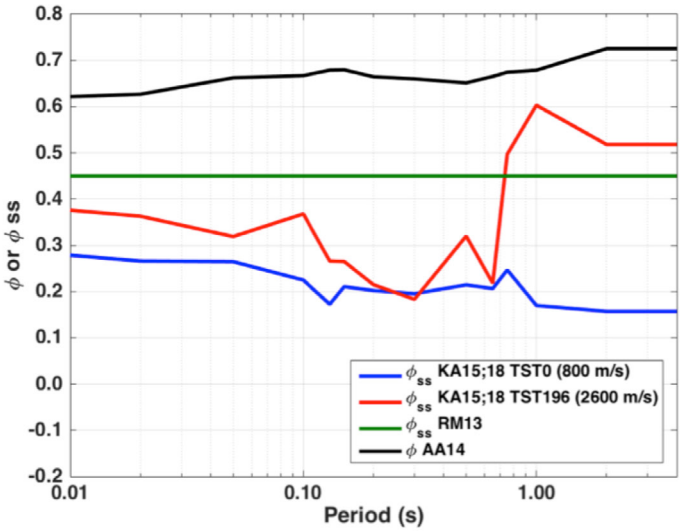

(b)

Fig. 6 - Site-specific residuals calculated at stations TST_0 and TST_{196} by Ktenidou et al., 2015a, 2018 (KA15;18) with respect to the AA14 GMPE (Akkar et al., 2014): (a) site terms $\delta S2S_s$, estimated for stations TST_0 (blue) and TST_{196} (red) with the AA14 site term accounting for V_{S30} (WIST, solid lines), or without the site term, i.e., with respect to standard rock 800m/s (WOST, dotted lines). (b) Standard deviation of the within-event term (φ) and standard deviation of the site specific within-event residual term (ϕ_{ss}).

Table 4 - Site terms (δS2Ss) used in this study. Residuals based on Akkar et al., 2014 GMPE as derived by Ktenidou et al., 2015a, and corresponding to a natural logarithm scale.

Period (s)	δS2Ss $TST_{0\text{-}WIST}$	δS2Ss $TST_{196\text{-}WIST}$	δS2Ss $TST_{0\text{-}WOST}$	δS2Ss $TST_{196\text{-}WOST}$
0.00	0.285	-0.442	0.8708	-0.5628
0.01	0.231	-0.393	0.8124	-0.5133
0.02	0.199	-0.359	0.757	-0.4742
0.05	0.510	-0.639	0.8062	-0.6999
0.10	0.412	-0.714	0.7892	-0.7914
0.13	0.262	-0.606	0.8169	-0.7209
0.15	0.146	-0.580	0.8198	-0.7193
0.20	0.088	-0.366	0.9982	-0.5535
0.30	0.081	-0.242	1.2327	-0.4794
0.50	0.006	-0.137	1.3249	-0.4091
0.65	-0.038	-0.250	1.3332	-0.5324
0.75	0.000	-0.166	1.4054	-0.4563
1.00	-0.061	0.057	1.3521	-0.2348
2.00	-0.026	0.110	1.2429	-0.1519
3.00	-0.026	0.110	1.2429	-0.1519
4.00	-0.026	0.110	1.2429	-0.1519

i.e., the variability of the site amplification around $\delta S2S_s$. The total standard deviation can thus be expressed as:

$$\sigma = \sqrt{{\phi_{S2Ss}}^2 + {\phi_{SS}}^2 + \tau^2} \qquad \text{Eq. 12}$$

When the site term is estimated in a site-specific way (including the associated epistemic uncertainties), the total sigma may be replaced by the smaller, "single-station" sigma, which does not have to account for the site-to-site variability:

$$\sigma_{ss} = \sqrt{{\phi_{SS}}^2 + \tau^2} \qquad \text{Eq. 13}$$

In such a case, the site-specific uniform hazard spectrum, $UHS_{Site\text{-}specific}(T)$, can be derived by adjusting the "reference" UHS obtained with the single-station variability with the site-specific amplification factor AF_s, as follows:

$$UHS_{Site-specific}(T) = UHS_{\sigma_{ss}(GMPE)}(T) \cdot AF_S(T) \qquad \text{Eq. 14}$$

Application to Euroseistest: Single-station variability

Table 5 lists the value of ϕ_{SS} for the two locations TST_0 and TST_{196}, as derived by Ktenidou et al. (2018) from weak to moderate motions recorded at these stations (PGA < 1 m/s²). These within-event variabilities are compared to the total standard deviation ϕ in the GMPE Akkar et al. (2014), as well as to the average ϕ_{SS} value proposed by Rodriguez-Marek et al. (2013) from an analysis of a large database of ground-motions from different regions (California, Switzerland, Taiwan, Turkey and Japan), which may be used as a default value when no site-specific estimate is available. Figure 6b displays these ϕ_{SS} values with respect to the oscillator period. These single-station variabilities are much lower than the AA14 total within-event standard deviation, over the whole period range at TST_0 and mainly at short to intermediate periods for TST_{196}. They are also generally smaller than the 0.45 average value proposed by Rodriguez-Marek et al. (2013), except at long periods for TST_{196}. These rather large ϕ_{SS} values at TST_{196} might be related with the relatively limited dataset over which these statistics could be derived (limited range in magnitude and distance of events). The recordings used correspond only to low-to-moderate magnitude events, with a site response always in the linear domain (see Ktenidou et al., 2018, and Bard et al., 2020, for more details). Nonetheless, several past studies suggest that ϕ_{SS} from strong motion data tends to be smaller than ϕ_{SS} from weak motion data (Abrahamson & Sykora., 1993; Toro et al., 1997). Using these single station sigmas at Euroseistest will lead to a reduction of hazard, with respect to hazard calculated with the total sigma. As the ϕ_{SS} values might be overestimated at long periods (above 1.0 s), these hazard estimates may be considered as upper bounds.

REFERENCE-ROCK HAZARD ESTIMATES AT EUROSEISTEST

This section presents the UHS estimated at the down-hole reference site TST_{196} for a 5000 year return period, with a discussion of the respective impacts of the single-station sigma, the rock-to-hard rock correction and the depth correction. All the PSHA computations (for rock and generic sites as well, level 0a) were performed with the OpenQuake engine which is now widely used worldwide probably because of its free availability and of its various characteristics as presented in Pagani et al. (2014).

Table 5 - Values of total (ϕ) and within-event (ϕ_{ss}) variabilities considered in this study.

Period (s)	Akkar et al., 2014 (AA14)	Rodriguez-Marek et al., 2013 (RM13)	Ktenidou et al., 2015a; 2018 residuals, estimated with respect to Akkar et al., 2014 GMPE. (KA15;18)	
	ϕ	ϕ_{ss}=0.45	ϕ_{ss} (TST_0)	ϕ_{ss} (TST_{196})
0.00	0.6201	0.45	0.2509	0.353
0.01	0.6215		0.2787	0.376
0.02	0.6266		0.266	0.363
0.05	0.6622		0.2647	0.319
0.10	0.667		0.2249	0.368
0.13	0.6789		0.1724	0.266
0.15	0.6796		0.2107	0.265
0.20	0.6645		0.2021	0.215
0.30	0.6599		0.1953	0.183
0.50	0.6512		0.2145	0.32
0.65	0.6652		0.2065	0.218
0.75	0.6744		0.2469	0.497
1.00	0.6787		0.1698	0.603
2.00	0.7254		0.1569	0.518
3.00	0.7254		0.1569	0.518
4.00	0.7254		0.1569	0.518

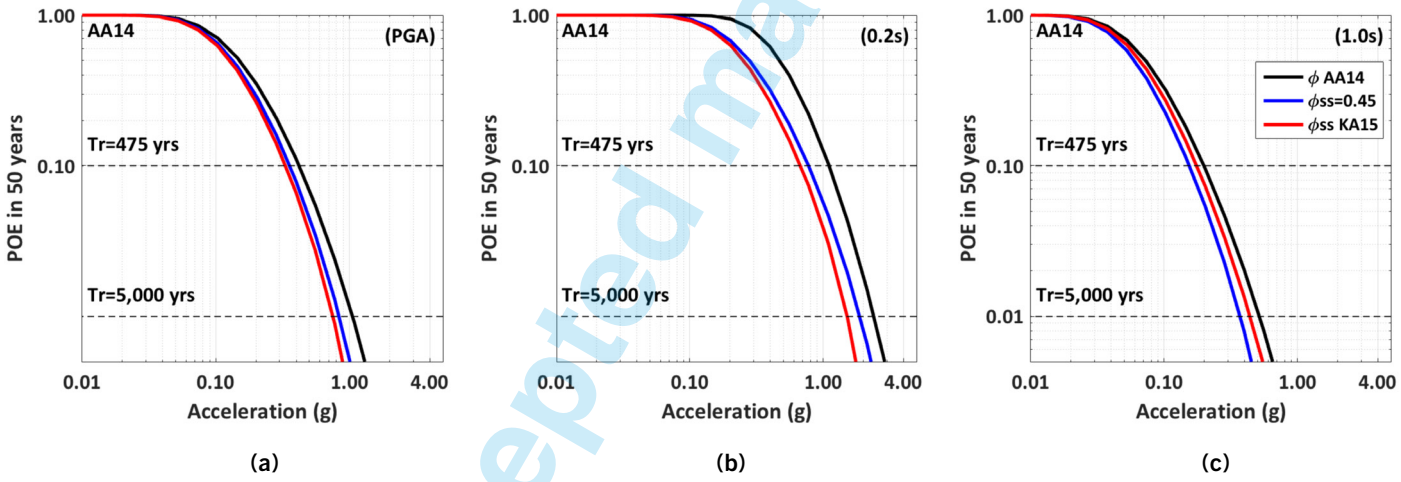

Fig. 7 - Impact of the single-station within-event variability (ϕ_{ss}) on the hazard curve at TST_0 station for three different spectral periods (PGA, (a); 0.2 s, (b); and 1.0 s, (c)). Calculations were performed using Akkar et al., 2014 GMPE on standard-rock (V_{S30}=800 m/s) and three different values for the within-event variabilities (ϕ). Black: period-dependent, ergodic, ϕ, from Akkar et al., 2014 (AA14); blue: constant partially non-ergodic, default value ϕ_{ss}=0.45 from Rodriguez-Marek et al., 2013 (RM13); red: period dependent partially non-ergodic, ϕ_{ss} from Ktenidou et al., 2015a;2018 (KA15).

Impact of single-station within-event sigma on hazard estimates (Standard rock 800m/s)

The impact of different within-event variabilities on the hazard curves is displayed in Figure 7. Hazard curves are evaluated at an outcropping standard rock with V_{S30} = 800 m/s, (i.e., a virtual reference site located at the same coordinates as TST_0 and TST_{196}) for different oscillator periods, considering alternatively the total sigma in the Akkar et al. (2014) GMPE, or a single-station sigma including the within-event variability evaluated by Ktenidou et al., (2015a, 2018) as well as Rodriguez-Marek et al. (2013). Figure 8a displays the corresponding UHS for a 5000 year return period. As expected, the hazard decreases with decreasing ϕ_{SS} values. Using the default ϕ_{SS} value (0.45), this decrease is about 20 – 25% at 5,000 year return period, while it may reach up to 40 % at some intermediate periods with TST_{196} ϕ_{SS} values. The high TST_{196} ϕ_{SS} values at long periods lead to a significantly smaller decrease, especially around 1 s. The variability between UHS obtained with default and site-specific ϕ_{SS} values is somehow limited and is generally around 10%. Considering default values derived from larger data sets may be a viable option on the safe side.

In all site-specific calculations that follow, the ϕ_{SS} values indicated in Table 5 derived from Ktenidou et al. (2015a) will be used.

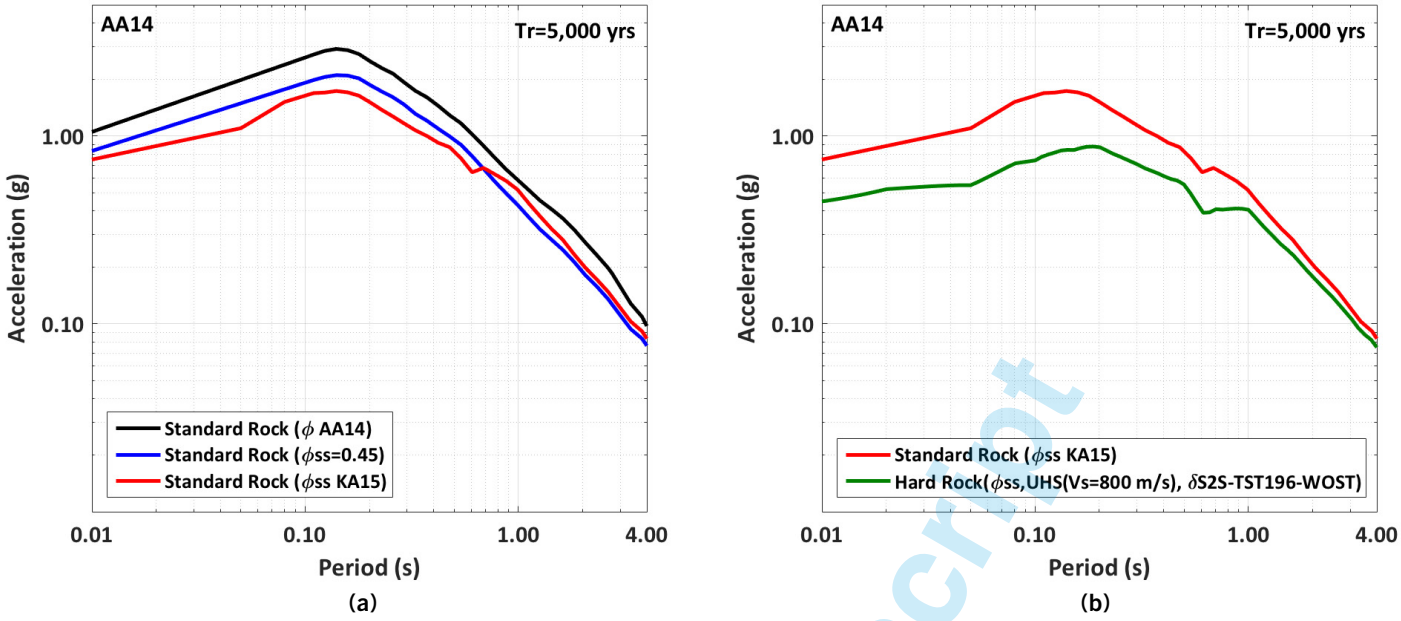

Fig. 8 : Euroseistest site, TST site, UHS at 5000 years return period: (a) Calculation for standard outcropping rock at TST site, impact of the single-station within-event variability (ϕ_{ss}) on the UHS for three different values of ϕ_{ss}; (b) Scaling of the UHS on standard outcropping rock (red) by applying the site term (δS2Ss), using $\phi_{ss\ KA15}$ to obtain the UHS on hard rock at depth (green, TST_{196} station).

UHS scaling for down-hole hard-rock TST_{196}

The next step is to apply the corrections to transfer this single-station hazard from standard outcropping rock to a downhole hard-rock with V_{S30} = 2600 m/s.

Application of site residual

The first and simplest way is to apply the TST_{196} site-specific residual according to:

$$UHS_{Hard\ Rock}(T) = UHS_{Rock(\sigma_{ss},\ Vs=800m/s)}(T) \cdot exp^{\delta S2S_{TST196,WOST}(T)} \quad \text{Eq. 15}$$

where σ_{ss} and $\delta S2S_{TST196}$ are GMPE dependent.

The results are displayed in Figure 8b for the Akkar et al. (2014) GMPE. The UHS at deep hard rock station TST_{196} are obtained by scaling the UHS on standard rock estimated with single station sigma ($\phi_{ss\ KA15,}$ Table 5), with the site term $\delta S2S_{TST196}$ estimated with respect to Akkar et al. (2014) GMPE (Table 4). The correction is significant, especially at short periods (amplitudes on hard rock twice as low as on standard rock, in the period range 0.05 to 0.2 s).

One might question the reliability of the $\delta S2S_{TST196}$ values as they are derived from weak motion observations with PGA_{rock} < 0.1g, and used to scale a UHS with much larger accelerations. However, the likelihood of a nonlinear behaviour on rock sites is very low and is usually neglected, so that weak motion residuals may be considered representative also for much stronger motion.

Table 6 shows the impacts in terms of hazard reduction of the single station sigma correction and the $\delta S2S$ correction, expressed in % at three spectral periods (PGA, 0.20s, 1.0s), together with their range over the whole period range. The single station sigma effect correction is stronger than the $\delta S2S$ correction, among the studied periods.

Application of shear-wave velocity and depth corrections

Another way to obtain the UHS on hard rock is to apply κ and shear-wave velocity corrections (VSC-KC), as well as depth correc-

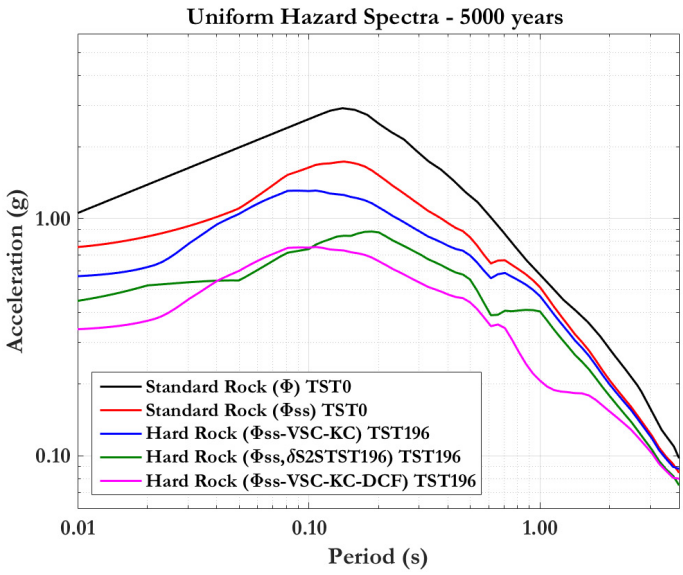

Fig. 9 - UHS at 5,000 years return period at station TST, Euroseistest, obtained with the AA14 GMPE for various types of reference rock sites. Black: standard, outcropping rock (V_{S30} = 800 m/s) with full sigma (σ); Red: standard outcropping rock (V_{S30} = 800 m/s) with single station sigma (σ_{SS}) proposed by Ktenidou et al., 2015a; Blue: hard outcropping rock (V_{S30} = 2600 m/s) with single station sigma (σ_{SS}) and VSC-KC correction; Magenta: hard rock at depth using the site residual ($\delta S2S_{TST196}$); Green: hard rock at depth (V_{S30} = 2,600 m/s) with single station sigma (σ_{SS}) and VSC-KC-DCF corrections. Impacts of the various corrections, expressed in %, are listed in Table 6 for three spectral periods (PGA, 0.15s, 1.4s).

tion (DCF) to the UHS on standard rock. The UHS on outcropping standard rock is estimated with Akkar et al. (2014) GMPE, either using total sigma σ (Figure 9, in black), or using single-station σ_{SS} (red). Then, by applying VSC-KC and DCF corrections to the UHS on standard rock, the UHS on deep hard rock may be obtained (magenta). To understand the relative effects of the VSC-KC and DCF corrections, the UHS corrected with VSC-KC only is also displayed (blue), while the corresponding values for three different periods are listed in Table 6.

The depth correction is stronger than the VSC-KC correction among all period ranges. The short period range is associated mainly to κ_0 effect (Figure 4a) which somehow "boosts" the short period and counterbalance the VSC effect, resulting in a very small VSC-KC correction. The intermediate period range (between 0.5 and 1.5 s) is associated to the destructive interference effects at depth (Figure 5). Combined, these two corrections result in hazard reductions between [8-45]% among all periods, that are approximately equal to the hazard reductions corresponding to the consideration of single station sigma σ_{SS} instead of total sigma σ [12-45]% (Figure 8a).

Comparison between both approaches

The UHS at TST_{196} station, located on hard rock at depth, is thus obtained either applying VSC-KC and DCF corrections to the UHS on standard rock (magenta curve in Figure 9) or by applying site residual scaling (green). The UHS obtained through these two different methods are rather close. The site residual correction ($\delta S2S_{TST196}$) lead to slightly larger values than the VSC-KC-DCF correction over most of the period range. The average difference is about 23% , but it reaches a factor of 2 around 1.0 s as a consequence of the destructive interference (at f_{dest} in the C2 correction). However, these relative differences remain relatively small compared to the overall correction from the outcropping standard rock (black and red curves) to the hard-rock down-hole location (magenta and green curves). At short and intermediate periods, the spectral accelerations obtained on hard rock at depth are much lower than the accelerations on outcropping standard rock (e.g. [0.66 – 0.87] g compared with [1.5-2.5] g at 0.2s). At long periods (larger than 1.0 s), the reduction in acceleration is lower.

As a conclusion, for this particular Euroseistest example, the reduction on rock hazard estimates is mainly due to single-station-sigma corrections (ϕ_{ss}) and to depth corrections (DCF), with smaller contributions of the host-to-target corrections (HTT, i.e. VSC-KC), because of the relatively large κ_0 value at hard rock (κ_t = 0.024 s). Single-station-sigma corrections and depth corrections are comparable in the short to intermediate period range, while at long periods the largest reduction comes for the reduced aleatory variability. The total reductions are very significant (up to a factor of 3 at some periods) and emphasise the importance of a careful assessment of the reference rock in site-specific hazard assessment studies. However, these conclusions might be different for another site (for instance with a hard-bedrock with a smaller κ_0 value), and could also be modulated would the epistemic uncertainty be considered in the different steps. One might question also the use of single-station variability UHS rock spectrum when using the Cadet et al. (2012a) depth correction, since the latter is mainly a generic correction tuned on the site-specific fundamental destructive frequency f_{dest}: part of the differences between magenta and green curves in Figure 9 might be related to this variability issue.

ESTIMATION OF SITE-SPECIFIC SURFACE HAZARD

The various approaches to include site effects into PSHA are now applied to the Euroseistest TST site, starting with generic or only partially site-specific approaches (level 0), and going on with site-specific approaches involving first a linear (level 1) and then a non-linear (level 2) site response (Table 1). For each approach, details are provided about their practical implementation and the associated issues, and the results are discussed and compared.

Level 0 - Generic or Partially Site-Specific Approaches

The site effects are accounted for in an average and approximate way through one or several site proxies.

Level 0a – use of site proxies in GMPEs

This is the simplest (and most widely used) approach, which consists in assuming that the actual amplification at the site of interest can be reasonably approximated by the site term of the GMPEs used in the hazard estimation. In other words, the specific

Table 6 - Impacts in terms of hazard reduction of the various corrections, expressed in %, at three spectral periods (PGA, 0.20s, 1.0s), together with their range over the whole period range.

Period (s)	0.01 (PGA)	0.2	1.0	[0.01-4.0]
5.2.1 Application of site residual				
Single Station Sigma (SSS)	28%	40%	12%	[12-41] %
DCF Site Residuals (δ_{S2S})	29%	26%	18%	[9-36] %
SSS & DCF	57%	65%	30%	[23-71] %
5.2.2 Application of shear-wave velocity and depth corrections				
Single Station Sigma (SSS)	28%	40%	12%	[12-41] %
VSC-KC	18%	16%	7%	[-3-18] %
DCF Cadet et al., 2012b	21%	18%	45%	[8-45] %
SSS & VS-KC & DCF	67%	74%	64%	[18-75] %

response of the site under study is assumed to be satisfactorily captured by the average site amplification of all stations in the GMPE strong-motion database exhibiting similar values of the site proxy. It should be noted that this approach ignores virtually almost all the site-specific information, especially if the site proxy has only a limited physical relevancy. Such an averaging over many sites therefore results in a relatively imprecise and generic assessment of the hazard, associated to a relatively large site-to-site variability, which must therefore be estimated with the full aleatory variability of the GMPEs. Nevertheless, as the hazard is computed on a specific site, another option could be to follow the approach proposed in Abrahamson et al. (2019), i.e. considering a non-ergodic GMM (such as Kotha et al., 2020 and Weatherill et al., 2020) with full consideration of the epistemic uncertainties on the non-ergodic source, path and site terms. Such non-ergodic GMMs were unfortunately not yet available for North-Eastern Greece at the time of the present study.

The most common proxy used to describe site conditions in GMPEs is the shear wave velocity of the top 30 meters, V_{S30}. Other proxies in use are the fundamental frequency, $f_{0,}$ (very rarely used as a continuous parameter), the site class (based on V_{S30} and/or f_0 ranges), and the depth at which the shear wave velocity first exceeds a given threshold, for instance 1.0 km/s or 2.5 km/s ($Z_{1.0}$ and $Z_{2.5}$, respectively). Some GMPEs use a combination of two proxies (e.g., V_{S30} and $Z_{1.0}$) in view of capturing different characteristics of the site amplification. The depth proxies ($Z_{1.0}$, $Z_{2.5}$) are usually not considered as a single site proxy in a GMPE, but they are used complementarily with V_{S30} in order to account for the site amplification due to deep sediments in general, also improperly called "basin effects".

Eight GMPEs are used here: the four active shallow crust GMPEs selected for the SHARE European Model (Akkar & Bommer 2010, AB10; Cauzzi & Faccioli 2008, CF08; Chiou & Youngs 2008, CY08; Zhao et al. 2006, ZA06), and their updated versions (Akkar et al., 2014, AA14; Cauzzi et al., 2014, CA14; Chiou & Youngs 2014, CY14), except for Zhao et al. (2006). The NGA2 model, Boore et al. (2014) (BA14), was also considered. The standard rock and soil hazard curves were calculated at the surface site TST_0, for three different spectral periods (PGA, 0.2s and 1.0s) using V_{S30}=186 m/s.

The hazard curves calculated at TST site are displayed in Figure 10, for standard rock (V_{S30} = 800 m/s) and for V_{S30}=186 m/s, the actual TST_0 site proxy value, and for three different oscillator periods (PGA, 0.2 and 1.0 s). The dispersion of hazard estimates is much larger on soil than on rock, for probabilities of exceedance (POE) lower than 0.1 over 50 years (return periods larger than 475 years). The epistemic uncertainty associated to the GMPE selection is much larger for soft sites than for (standard) rock sites. This variability has thus been quantified as the ratio between the largest and the lowest accelerations among the 8 values predicted by the GMPEs (See Table 7, for 0.1 and 0.01 probability of exceedance over 50 years). The dispersion in general increases with the return period and decreases with soil stiffness.

This dispersion is due to the diversity of site terms from one GMPE to the other. Figure 11, shows the ratios obtained by divid-

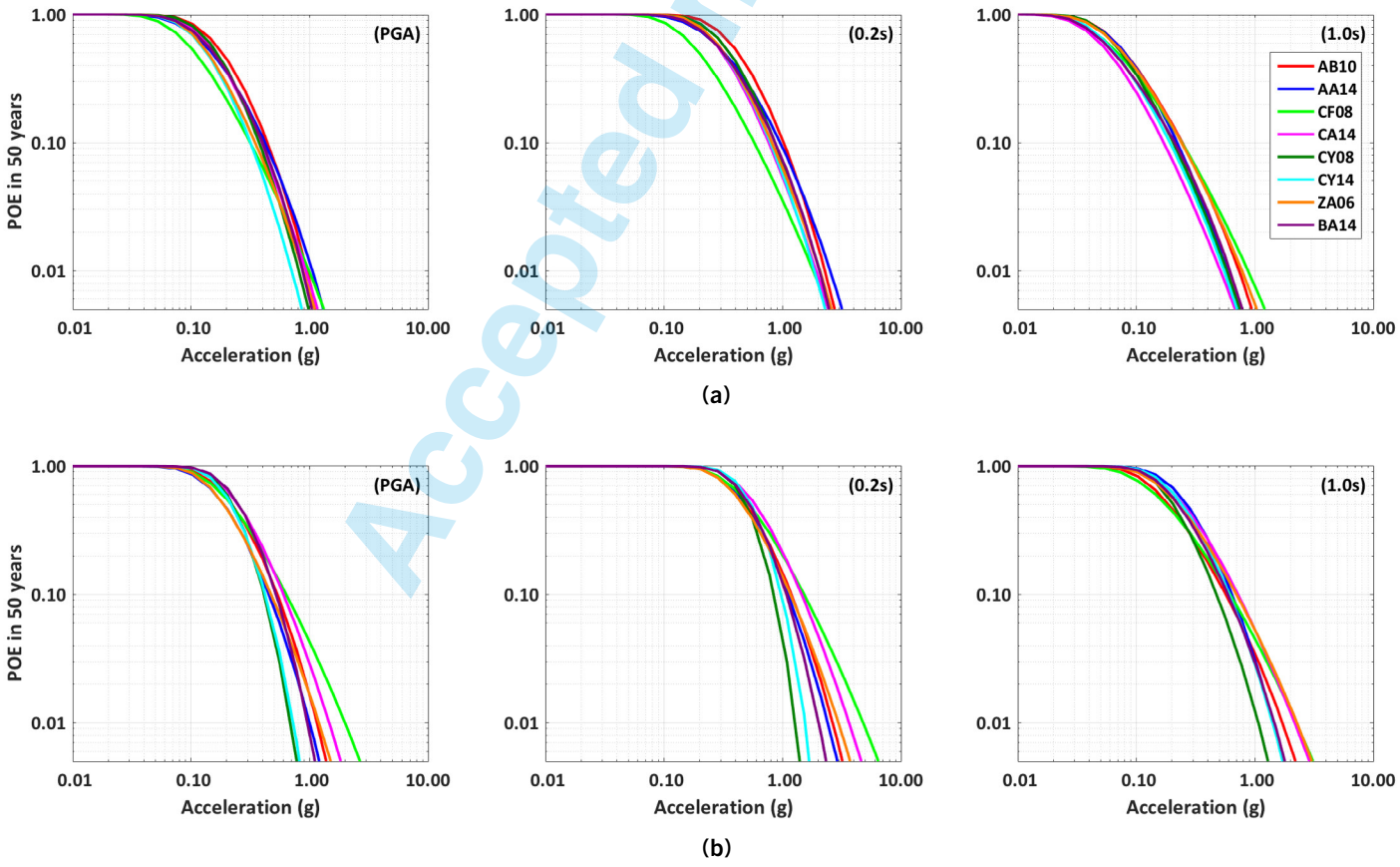

Fig. 10 - Hazard curves calculated at TST site, at the middle of the Euroseistest basin using 8 different GMPEs: (a) Standard rock (V_{S30}=800 m/s); (b) Soil (V_{S30}=186 m/s). See the text for further explanations.

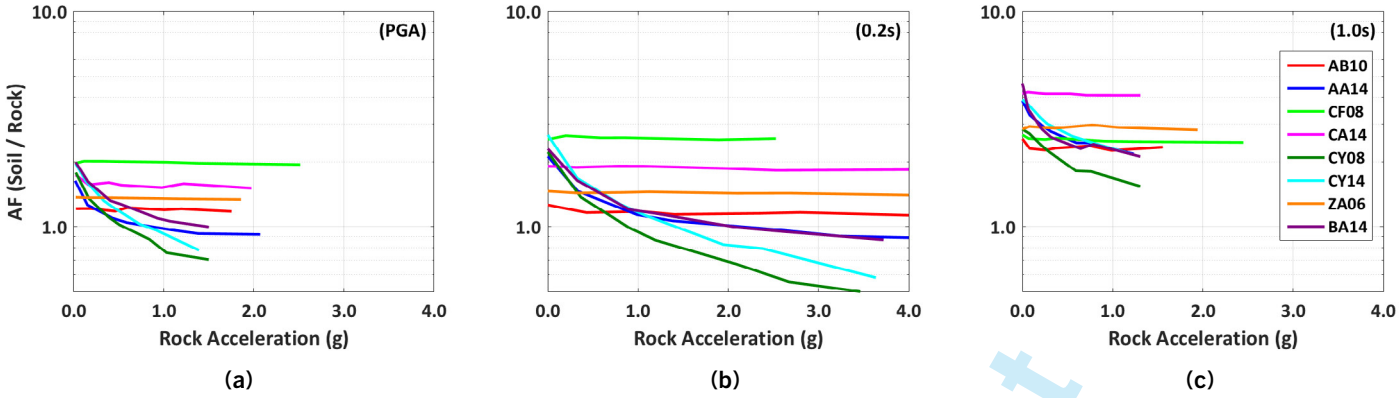

Fig. 11 - Evolution of the GMPE site term (i.e., ratio of the spectral acceleration on soil with respect to rock spectral acceleration for the same return period) with the reference rock motion for the eight selected GMPEs, for three oscillator periods (PGA, (a); 0.2 s, (b); 1.0 s, (c)).

Table 7 - Ratio between the larger and the lower accelerations, among the 8 values obtained with the 8 different GMPEs, on rock and on soil (bold italic). POE = probability of exceedance over a 50 years life time.

POE	Return period (years)	PGA		Sa (0.2s)		Sa (1.0s)	
		Rock	Soil	Rock	Soil	Rock	Soil
0.1	475	1.41	1.55	1.78	1.70	1.43	1.49
0.01	4975	1.46	2.76	1.38	3.42	1.73	2.15

ing the acceleration predicted on soil by the acceleration predicted on rock for the same return period (Sa_{soil} / Sa_{rock}). For AB10, CF08, ZA06 and CA14, these ratios remain mostly constant and above 1.0, whatever the hazard level. These GMPEs predict linear behavior with systematic amplification at all return periods (all acceleration levels) and for the three spectral periods. On the other hand, for AA14, CY08, CY14 and BA14, the ratios decay with increasing return period (increasing level of acceleration) for the three different spectral periods. These models include a nonlinear component in the site term (as shown for instance in Eq. 10 for the AA14 case). The large impact of the GMPE selection on soft soil hazard curves is thus mainly due to the variability of the GMPE site terms: some of them are only data driven, others are partially constrained by 1D numerical simulations.

This simple test demonstrates the high level of epistemic uncertainty linked with the site term in the generic PSHA approach, drawing the attention on the large differences between linear and non-linear models. One immediate conclusion is that hazard studies for soil sites should include a careful analysis of their site terms, to ensure that the whole range of epistemic uncertainties is captured.

However, as the goal of the present study is mainly methodological to illustrate the sensitivity of site-specific PSHA to the selected approach, and not to achieve a complete site-specific PSHA study at Euroseistest, we will limit the rest of the paper to the use of one single GMPE. The comparison in Figure 11 indicates that the AA14 GMPE can be considered a good choice, since it lies in the middle of other models, while also involving a non-linear site amplification model. Another advantage is that its standard deviation σ is separated in between event (τ) and within-event terms (ϕ), which is a requirement for using single-station sigma (σ_{ss}) in PSHA calculations. Moreover, this GMPE was in the short list of equations selected for crustal earthquakes in the GEM project (Stewart et al., 2015).

Finally, using the selected AA14 GMPE, the hazard disaggregation at TST rock site is performed for the 5000 year return period at three different spectral periods (PGA, 0.2s and 1.0s, see Annex A). The results indicate a major contribution from magnitudes Mw=[6.0-7.0] and short distances (Rhyp=[0-20] km). This information will be used whenever (magnitude, distance) pairs that contribute most to the hazard are required for some site-specific approaches.

Level 0b – A posteriori modification of the site term using a "SAPE"

This approach requires a further methodological step with respect to Level 0a. The simple site amplification term embedded in GMPEs may be considered as a first-order model for the target site response, but some additional site-specificity can be included to improve its description. An independent site correction factor can be applied as a post-processing to the rock uniform hazard spectrum (UHS). In other words, the idea is to estimate the hazard curve on rock and handle the site term through specific Site Amplification Prediction Equations (SAPEs). The SAPE concept was introduced by Cadet et al. (2012a, b) to allow the estimation of site amplification to be fully independent of the GMPE derivation, thus avoiding any possible trade-off with source or path terms. In principle, in the long run, the use of SAPEs could allow to account also for other kinds of site effects, such as surface or subsurface geometry (aggravation factors for topography or basin effects, see Chavez-Garcia & Faccioli 2000, Riga et al., 2016 or Boudghene-Stambouli et al., 2018), or nonlinear effects (Derras et al., 2020), in a more physical - though still simplified - way than what is currently proposed in most recent GMPEs.

Amplification factors were derived by Cadet et al. (2012a, b) from the recordings at a large number of Japanese KiK-net sites, corrected to be normalised with respect to a standard rock, and correlated with some sets of site parameters to establish "stand-alone" site amplification factors. SAPEs have been developed considering different proxies: the travel-time average S-wave velocities over the top z meters (V_{SZ}, with z =5, 10, 20 and 30 m), and the fundamental frequency f_0. The SAPEs were calculated for each individual proxy (V_{S5}, V_{S10}, V_{S20}, V_{S30}, f_0) and for all proxy pairs ($f_{0, VSZ}$). The correlation between the considered pairs ($f_{0, VSZ}$) and the amplification factors were derived in the dimensionless frequency (f/f_0) domain. The best performance in predicting site amplification was obtained with the pair $V_{S30 - f0}$, while the best single parameter proved to be f_0 and V_{S30}, in agreement with a few other studies (Luzi et al., 2011). Some recent papers consider more elaborated site proxies (Derras et al., 2016; Boudghene-Stambouli et al., 2017; Bergamo et al., 2020, 2021), but they have not been considered for the present methodological study as the corresponding functional forms, derived using a neural network approach, are much more complex. They are however a serious option for any site-specific study, and this kind of machine learning tools will certainly allow significant improvements in the near future.

The UHS on soil can be obtained from the UHS on standard rock as expressed in Eq. 16, where the *j* index stands for the various expressions of SAPEs proposed in Cadet et al. (2012b), depending on the used proxies.

$$UHS_{soil}(\mathrm{T}) = UHS\ (T)_{(\mathrm{VS30}=800\ m/s)} \cdot SAPE_{\ j}(T) \qquad \text{Eq. 16}$$

The different site proxies required for the application of the SAPE approach are therefore V_{S5}, V_{S10}, V_{S20}, V_{S30}, f_0 , and their values at Euroseistest are, respectively, 144, 153, 170 and 186 m/s, while the fundamental frequency is 0.7 Hz. The corresponding SAPEs are shown in Figure 12a. They do exhibit some variability, which however remains smaller than the dispersion obtained by applying different GMPEs (Figure 11 and Table 7), even when considering only linear GMPEs. As expected, the amplification factor is maximum at the fundamental frequency $f_{0.}$ It reaches 4.8 for the SAPE based on the ($f_{0, VS30}$) pair (which is selected in the following for comparative purposes as it was identified as the best performing pair), while it is 3.6 for the ($f_{0, VS5}$) pair. The resulting UHS on soil are displayed in Figure 12b, together with the standard rock reference, and the UHS obtained with VS_{30} of 186 m/s accounted for in the GMPE (generic approach, see Section 6.1.1). The SAPE approach results in significantly larger hazard estimates at the surface (e.g. 4-5g rather than 2-3g at 0.1s). Such values are very high, probably too high, and are due to the non-consideration of non-linear site response by Cadet et al. (2012b). This should certainly be corrected in the future; however, one may notice that even for weaker motion whether the soil behavior can be considered essentially linear, GMPEs predict less amplification than SAPEs, especially around the fundamental period, because their V_{S30} basis does not allow to account for resonance phenomena.

Level 1: site specific, linear

Quick overview

The term "site-specific" implies that the site is well characterised (i.e., knowledge of the velocity profile, of the geotechnical parameters, of the 2D or 3D underground structure, among others) and/or it is equipped with instruments that provide high quality recordings, so that the actual site amplification can be estimated either in a purely instrumental way, or with numerical simulation. Level 1 approaches are the simplest "site-specific" approaches

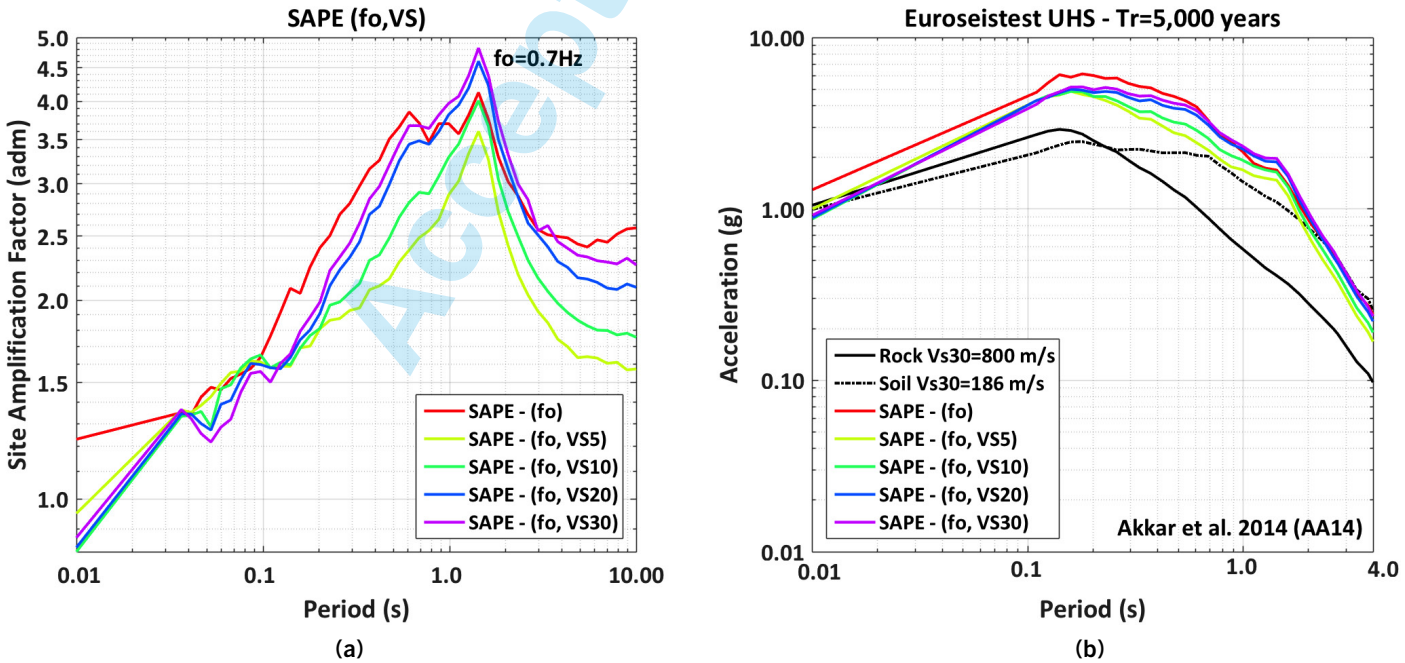

Fig. 12 - (a) Site amplification factors estimated at TST_0 station from site amplification prediction equations (SAPEs, Cadet et al., 2012b) with different proxies; (b) Corresponding 5000 years UHS using Akkar et al., 2014 GMPE and the various SAPEs.

where the site amplification can be applied as a post-processing since the site response is considered linear (i.e., independent of the rock motion level). This is generally the case of stiff/hard materials mostly with linear elastic behavior, or soft materials with elastoplastic nonlinear behavior under weak ground-motion only. However, this is not the case of Euroseistest, corresponding to a soft soil in a rather active area, where non-linear site response is expected at moderate to long return periods. Such linear results are shown here mainly for a methodological purpose, to illustrate how the site-specific results can vary depending on the approach.

Under linear site response assumption, the surface hazard may be computed with the hybrid probabilistic method, which consists in multiplying the UHS on rock by the linear amplification function (Eq. 17), $AF_{lin}(f)$ (Equivalent Approach 1 or Approach 2, NUREG 6728) :

$$UHS_{soil}(f) = UHS_{Rock}(f) \cdot AF_{lin}(f) \qquad \text{Eq. 17}$$

There are several variants of this approach, depending on the location and nature of the reference site (requiring or not some corrections for rock stiffness or location at depth), the way the site amplification is estimated (instrumental or numerical), and the spectral domain (Fourier or response spectra) where it is estimated.

Level 1a – Linear Site Response with Site-specific Residual scaling (Response spectrum domain)

As indicated in Section 4.1.1 dealing with "hard-rock" corrections, sites with a large enough number of ground-motion recordings offer the possibility to estimate their site–specific amplification through their site-specific residuals $\delta S2S_s$ and the associated standard deviation ϕ_{ss}, with respect to the GMPE used to determine PSHA. Such a site-specific bias ($\delta S2S_s$) may then be used to correct the GMPE predictions for the site under consideration. Furthermore, the replacement of a generic estimate by a site-specific estimate, may allow, in principle, to replace the total within-event residual standard deviation (ϕ) by the single-station within-event variability (ϕ_{ss}) of the site. This latter possibility should however be considered with caution as detailed below.

As mentioned previously, there are two possibilities to estimate a site residual for a given GMPE: either with respect to the motion prediction including the site term ("WIST"), or without it ("WOST"), i.e., with respect to standard rock conditions. The UHS at the soil surface (TST_0) can thus be obtained in two different ways:

- Case 1 (WIST):

The UHS predicted on soil with the site characteristics (here V_{S30} = 186 m/s), $UHS_{Soil(\phi,\ Vs=186m/s)}$, must be corrected with the site residual $\delta S2Ss_{TST_0,WIST}(T)$

$$UHS_{TST_0}(T) = UHS_{Soil\,(\phi,\ VS30=186\ m/s)}(T) \cdot exp^{\delta S2Ss_{TST_0,WIST}(T)} \qquad \text{Eq. 18}$$

Note that in this case (Eq. 18), the reference hazard is computed with the full variability (σ) of the GMPE and not the single station one (σ_{SS}). The site term in AA14 GMPE includes a linear and a non-linear component, which are calibrated on the sole basis of the generic proxy V_{S30}. The $\delta S2Ss_{TST_0,WIST}$ correction is ground-motion independent and based on weak motion data only (Ktenidou et al., 2015a, 2018), therefore only the linear site term can be considered as site-specific, while the non-linear dependence remains generic. Therefore, the site-to-site variability to be considered should in principle be somewhere between the full variability and the single-station one. Nevertheless, as the available information for the used GMPE is insufficient to clearly distinguish the respective parts of variability due to linear and non-linear components, and as the latter is very significant for the large return period considered here, we decided to stay on the safe side by considering the full variability associated to a generic site term.

- Case 2:

The other option is to correct the UHS predicted on standard rock, with the site residual $\delta S2Ss_{TST_0,WOST}(T)$:

$$UHS_{TST_0}(T) = UHS_{Rock\,(\phi_{ss},\ VS30=800\ m/s)}(T) \cdot exp^{\delta S2Ss_{TST_0,WOST}(T)} \qquad \text{Eq. 19}$$

In the present case (Eq. 19), it is accepTable to estimate the reference (standard rock) hazard with the single station variability (σ_{SS}). In this case, the site response for standard rock conditions may be considered as only linear, so that the correction with the WOST residual may be considered as fully site-specific. The values of the site residuals $\delta S2Ss_{TST_0}$ (WIST and WOST cases) can be found in Table 4, and the values of the within-event variability ϕ and ϕ_{SS} in Table 5 (Figure 6b). The WIST and WOST amplification factors are plotted in Figure 6a as a function of frequency. The successive steps to follow for the WIST and WOST cases are detailed in Figure 13a and Figure 13b respectively and the corresponding amplification functions are shown in Figure 14a. The obtained UHS_{soil} are displayed in Figure 15b (red for WIST, green for WOST) where they can also be compared with level 0a and 0b results shown on Figure 15a. The accelerations obtained with WOST residual scaling are larger than the accelerations obtained with a WIST residual scaling, despite the consideration of smaller single-station sigma, mainly because of the inclusion of a strong non-linear site response term in the AA14 GMPE, while the $\delta S2Ss_{TST_0,WOST}$ site residual assumes de facto a linear site response.

Level 1b - Linear Site Response Analysis with Instrumental AF(f)

The site-specific amplification function, AF(f), may be obtained instrumentally in different ways:

- Comparing recordings at the site with recordings from a nearby "reference" site, through the Standard Spectral Ratios (SSR) technique introduced by Borcherdt (1970). This technique is usually applied in the Fourier domain, and evaluates the instrumental "Fourier transfer function". In the present case we used the SSR derived from Euroseistest accelero-

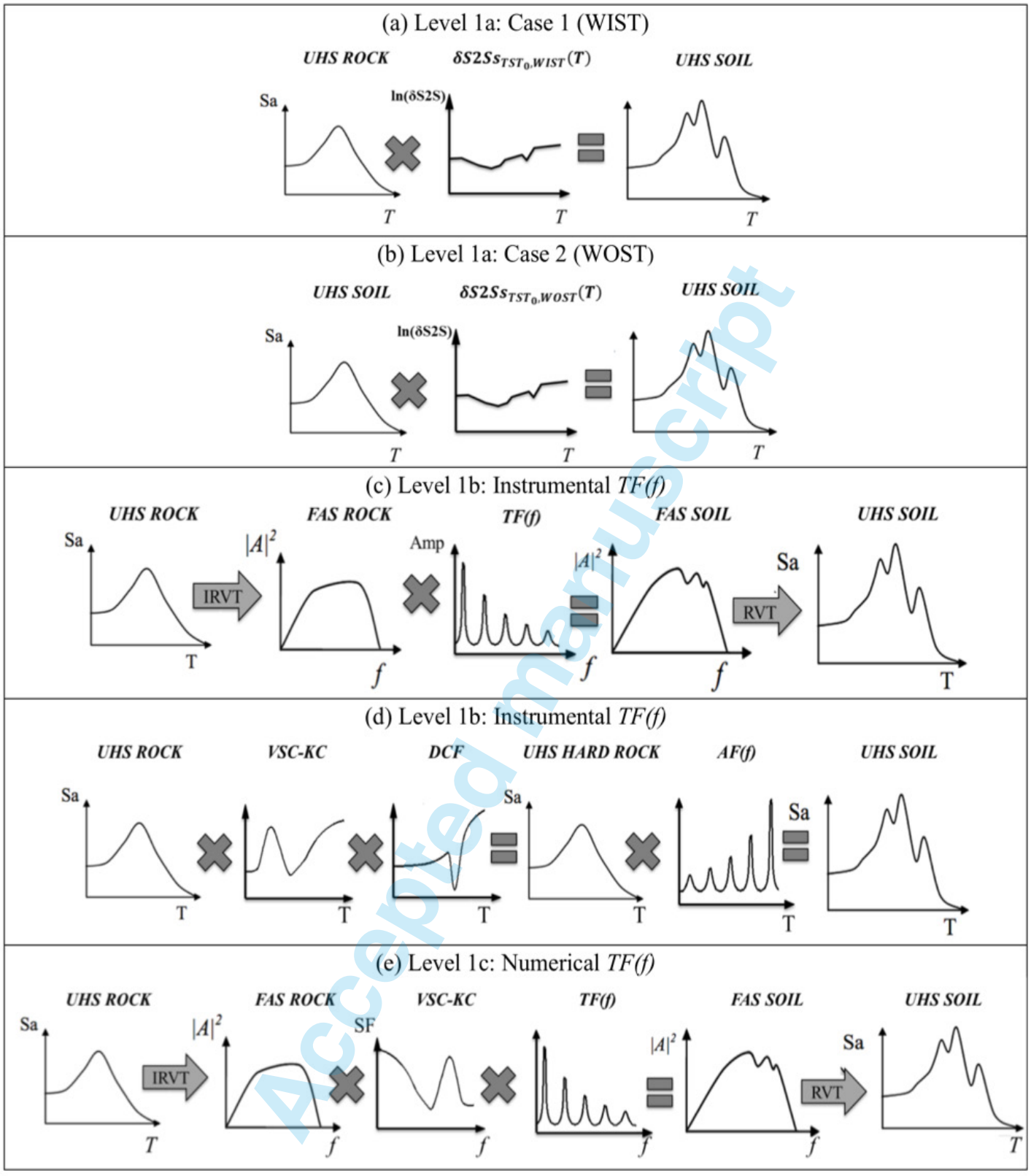

Fig. 13 - Procedures to obtain the site surface UHS for: (a) Level 1a, Case 1 WIST, the Amplification Function is available in the response spectra domain with respect to standard-rock condition; (b) Level 1a, Case 1 WOST, the Amplification Function is available in the response spectra domain with respect to soil condition; (c) level 1b, the Amplification Function is available in the Fourier domain with respect to standard-rock condition; (d) level 1b, the Amplification Function is available in the response spectrum using site residuals, with respect to hard-rock conditions at depth: the UHS on standard rock needs to be corrected (V_S-□ and depth) before applying the site amplification factor; (e) level 1c, the amplification function is computed numerically with respect to the down-hole site. (Modified from Rathje et al., 2005).

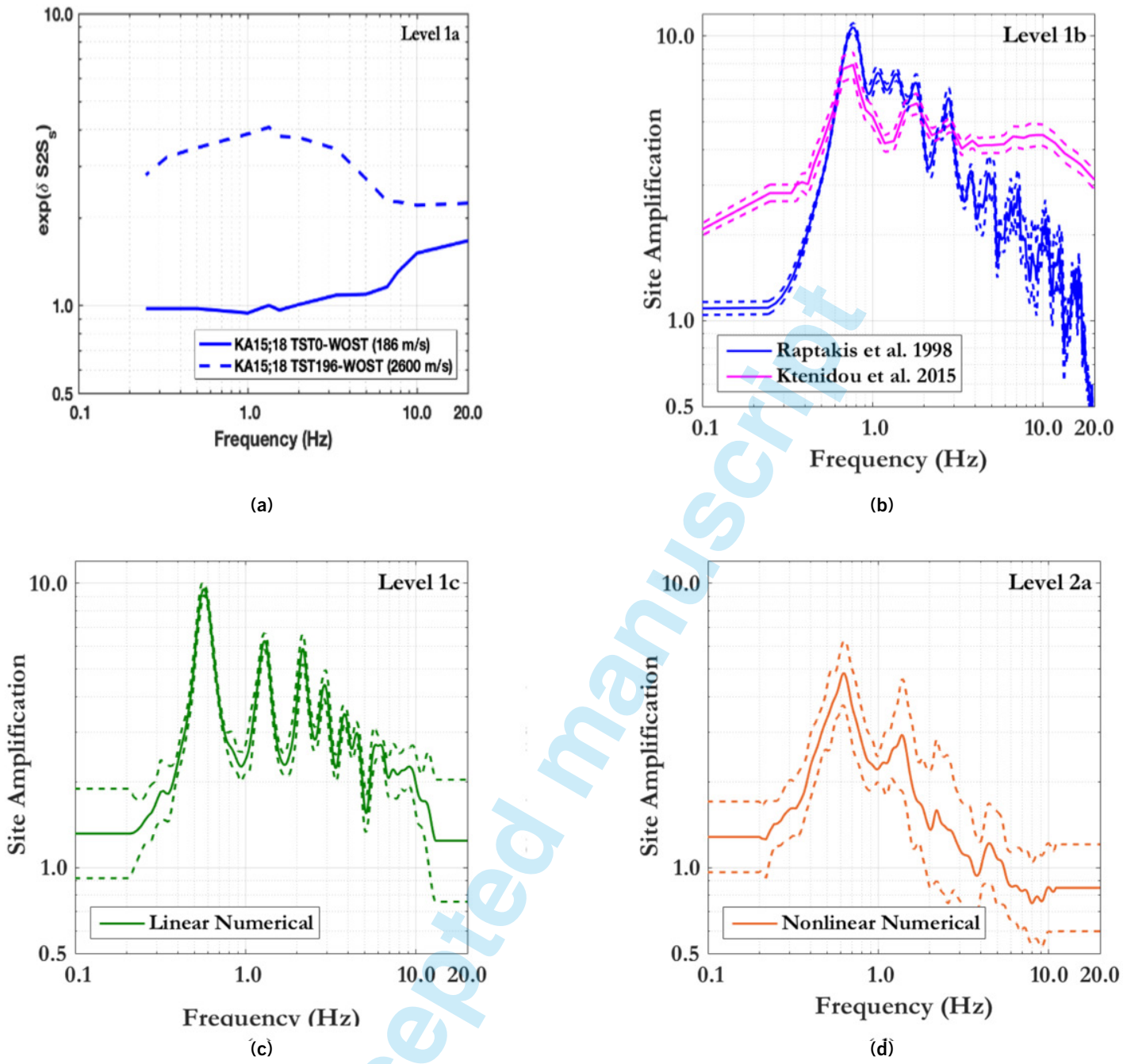

Fig. 14 - Linear Amplification Functions obtained for TST_0 for the different site-specific approaches at Euroseistest: (a) Level 1a – AA14 site-specific residual (response spectrum domain) for TST_0 with respect to the V_{S30} = 186 m/s prediction (WIST, solid line, case 1 in the text), and to the V_{S30} = 800 m/s standard rock (WOST, dotted line, case 2 in the text); (b) Level 1b – Instrumental site amplification obtained in the linear case with respect to a nearby outcropping rock (blue, Fourier domain) and with respect to the TST_{196} deep hard rock (magenta, response spectrum domain); (c) Level 1c –Fourier transfer function TF(f) obtained with 1D Linear numerical simulation with respect to outcropping hard-rock; (d) Similar to (c) in the non-linear case for input signals tuned to the 5000 year UHS at 2600 m/s outcropping rock.

metric data (Raptakis et al., 1998), considering the outcropping, standard-rock reference station (PRO) located on the northern valley edge (see Figure 1b).

- By generalised inversion techniques (GIT) involving a network of regional stations providing the site term with respect to one particular or a set of reference stations. Such techniques also generally operate in the Fourier domain. We did not use this approach in the present case, considering that previous comparisons have shown a good agreement between GIT and SSR techniques when the reference is the same (e.g., Andrews 1986, Riepl et al., 1998)
- Using local site-residual (*Eq. 20*), as described in section 6.2.2. This technique is similar to the GIT technique, except that it is in the response spectrum domain. We consider here the difference of "WOST" site residuals, between TST_0 and TST_{196}:

$$AF(f) = exp^{\delta S2Ss_{TST_0,WOST}(f) - \delta S2Ss_{TST_{196},WOST}(f)}$$ Eq. 20

The amplification functions obtained with the SSR and the site residual techniques are displayed in Figure 14b as a function of frequency. Their overall shapes are similar, but they cannot be directly compared since they correspond to two different spectral domains and two different reference stations.

- The higher AF values at low and high frequencies for the site-residual approach results from its operation in the response spectrum domain, where the low frequency asymptote is related to amplification on peak displacement, while the high-frequency asymptote is related to amplification on PGA. Both peak values are sensitive to amplification in other frequency bands, so that they may be significantly larger than 1.0. Conversely, in the Fourier domain, the PRO to TST_0 Fourier transfer function is very close to 1.0 at low frequency: wavelengths are too long to see any difference between PRO and TST_0 underground conditions). And it is below 1.0 at very high frequency because of the effects of damping in the 200 m thick sedimentary deposits.
- Similarly, the slightly lower amplification of the TST_0/ TST_{196} residual ratio around the 0.7 Hz fundamental frequency, comes from the inherent smoothing of the response spectrum approach, even though the reference rock is harder than for the PRO to TST_0 Fourier transfer function.

The site amplification relying on SSR technique is provided as a Fourier transfer function. The rock UHS must thus be first converted into a rock Uniform Hazard Fourier Amplitude spectrum (UHFAS), then the site amplification can be applied in the Fourier domain, and at last it is necessary to come back in the response spectrum domain. These conversions from the response spectrum domain to the Fourier domain, and vice versa, are performed using the Inverse Random Vibration Theory (IRVT) and the forward random vibration theory (RVT) (Campbell 2003; Al Atik et al., 2014). These techniques presented in section 4.1.1.2 dealing with V_S-κ corrections are applied here for the same scenario event and with typical duration values. The successive steps to follow are detailed in Figure 13a. In the residual approach, as the site amplification is provided in the response spectrum domain, it must be applied directly to the hard-rock UHS. When needed, V_S-κ and depth corrections must similarly be applied to the UHS on standard rock to obtain the UHS on hard rock (Figure 13d).

The resulting UHS at 5,000 years are shown in Figure 15b (SSR based in blue, residual based in magenta). They exhibit much larger differences than the corresponding amplification functions (Figure 14b), because of large differences in the reference rock UHS. The site residual approach leads to much lower values than the approach based on SSR, over the whole period range. Both reference rock corresponds to single-station PSHA estimates, however one is an outcropping standard rock (in the case of AF(f) based on the SSR technique), the other is a deep hard rock site (in the residual approach). As shown in Figure 9, the latter is much smaller than the former.

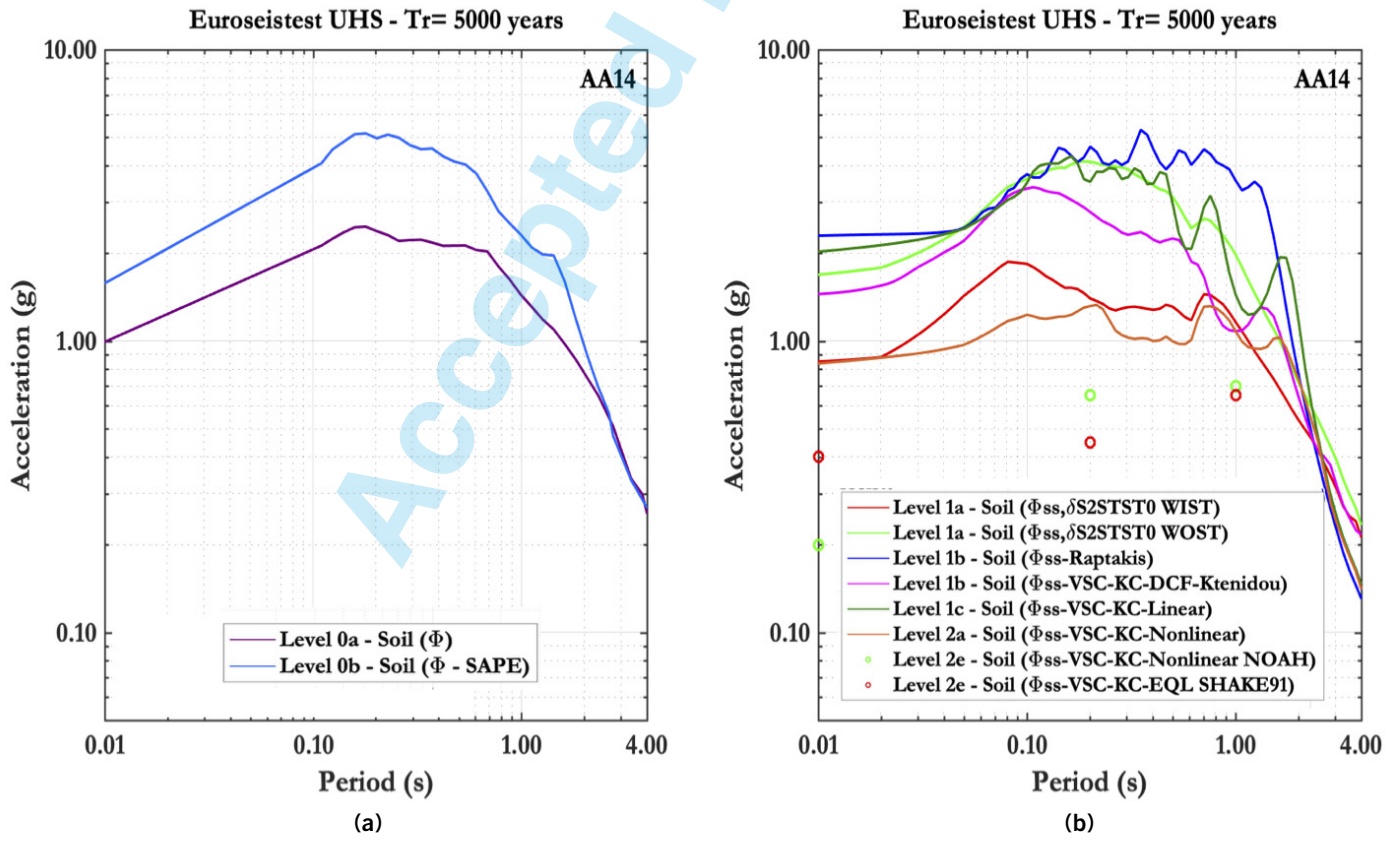

Fig. 15 - (a) Euroseistest UHS on soil from generic or partially site-specific approaches (level 0a and level 0b); (b) Euroseistest hazard spectra on soil for the hybrid site-specific hazard approaches (levels 1a, 1b, 1c and 2a); the additional symbols (open circles) stand for the Aristizabal et al., 2018b results.

Level 1c – Linear Site Response Analysis with Numerical AF(f)

The amplification function can be also estimated numerically. Here we only considered the 1D ground response, but the same approach could be used with 2D or 3D simulation codes, as done by Chavez-Garcia et al. (2000), Makra et al. (2016) or Maufroy et al. (2015, 2016, 2017). The linear 1D response has been computed using the time-domain code NOAH (Nonlinear Anelastic Hysteretic finite difference code, Bonilla, 2000), applied here in the linear domain with the velocity profile indicated in Figure 2, and considering outcropping hard-rock reference conditions (as usually done in numerical modelling techniques). The site amplification is thus provided here in the Fourier domain (as in level 1b, Figure 13c), which requires again a swap from the response spectrum domain to the Fourier domain. The procedure is illustrated in Figure 13e. The single-station sigma standard-rock UHS response spectrum is first corrected for V_S and kappa. The resulting response spectrum is transformed in the Fourier domain using IRVT (Al Atik et al., 2014), multiplied by the Fourier transfer function corresponding to the linear response of the 1D soil column, and then the surface response spectrum is derived from site surface Fourier spectra using forward RVT.

The level 1c 1D numerical transfer function is displayed in Figure 14c. The linear Fourier transfer function cannot be compared simply with the instrumental one in Figure 14b, since the reference is not the same: the instrumental AF is estimated with respect to outcropping rock (PRO station), while the linear numerical AF is estimated with respect to hard rock (TST_{196}). Nevertheless, the well separated resonance peaks in the numerical transfer function show that 2D and 3D effects are indeed ignored in these 1D approach. Such peaks can be identified also in the surface response spectrum displayed in Figure 15b (dark green curve). The UHS obtained is lower than the SSR-based level 1b UHS (blue) and higher than the residual-based level 1b UHS (magenta). The amplitudes are approximately comparable to the approach 1a based on residuals (site residual $\delta S2Ss_{TST_0,WOST}$, light green). Most of the differences between the various approaches come from the reference hazard (within - or outcropping conditions, standard or hard-rock).

Level 2: site specific, non-linear

Euroseistest is characterised by soft deposits and the site response is expected to be non-linear at least for long return periods. The amplification function AF(*f*) thus depends not only on the reference rock motion level S_{ar}(f), but also on the details of the time-history (e.g., its phase content) which partly controls the strain values. A given absolute level at site surface may be reached for different rock reference motion (corresponding to different return periods and / or different earthquake scenarios) and amplification levels corresponding to different non-linear site response. A full probabilistic estimate at soft sites should then couple the analysis of rock hazard and the distribution of conditional site amplification.

Following Bazzuro & Cornell (2004a, b), several approaches have been proposed to account for non-linear site response in probabilistic site-specific hazard calculations. They are labelled as sublevels 2a to 2e in Table 1 , which all involve an analysis of non-linear site response. They are briefly presented in this section. A nonlinear analysis could in principle be performed on an instrumental basis only, however it is not possible at Euroseistest since there are no recordings of strong enough motion. The non-linear site response is thus accounted for only with numerical simulation tools (NOAH and SHAKE codes), which are briefly presented. An overview is then given of the principles of the five "level 2" methods mentioned in Table 1, but only two of them could be applied here and give rise to specific results for Euroseistest.

Non-linear site response at Euroseistest

The nonlinear computations used here are detailed in Aristizabal et al. (2018b), a study dedicated to the comparison of two fully probabilistic site-specific approaches (levels 2b and 2c). Their basis is thus only shortly summarised; the interested reader should refer to Aristizabal et al. (2018a, b) for more details

We consider only 1D, 1-component site response analysis. Recent benchmarking studies (Stewart et al., 2008; Régnier et al., 2016b, 2018) recommend the use of several non-linear codes to better capture the associated epistemic uncertainty, however we have applied only one fully nonlinear code, the NOAH (Nonlinear Anelastic Hysteretic finite difference code, Bonilla, 2000) time-domain code. Our goal is not to propose a complete site-specific PSHA study at Euroseistest, but to illustrate how much the hazard results depend on the approach selected. Nonetheless, a linear equivalent approach (SHAKE, Schnabel et al., 1972) has also been considered for methods 2b and 2c.

The low-strain parameters of the soil column are described in Figure 2 and Table 2 (same as in level 1c). The non-linear parameters have been defined through the G/Gmax degradation curves and, when needed, the strength profile has been derived from the friction angle ϕ and K_0 (coefficient of earth pressure at rest) values, according to the user manual (Bonilla 2000). The computations were performed using the actual soil profile, with a reference motion being specified for hard-rock (V_{S30} = 2600 m/s), outcropping conditions. The corresponding rock hazard therefore includes only the VSC-KC corrections, without the depth correction (DCF).

Approaches for including non-linear site response in Site-specific PSHA

To perform a site-specific PSHA, there are two main approaches. The hybrid approach (level 2a) combines a probabilistic approach for the reference rock hazard and a deterministic approach for the site amplification, conditioned by the level of rock hazard. The fully probabilistic approach, first introduced by Cramer (2003), implies the convolution of a non-linear, rock-motion dependent, site-amplification function having its own distribution, with the hazard curve on rock. Several methods have been proposed for the practical implementation of this convolution.

- Hybrid approach

This approach is formally the same as the one considered in level 1c, except that the (deterministic) site amplification is tuned to the reference rock hazard level as follows (Eq. 21):

$$HS_{soil} = UHS_{Ref\_Rock(Surface,\ Borehole)} \cdot AF_{(Instrumental,\ Numerical)}(f, S_{ar}) \quad \text{Eq. 21}$$

The non-linearity of the site response is accounted for, but not its variability associated to the sensitivity to details (phase) ot the input rock time series. The resulting surface spectrum can no longer be considered as a uniform hazard spectrum associated to the return period of the rock reference. The exceedance probabilities may differ from one oscillator period to another because of the non-linear energy transfer process, and the replacement of a convolution by a simple multiplication may change the exceedance probability. The examples investigated in Bazzurro & Cornell (2004b) indicate that this hybrid method tends to be non-conservative at all frequencies and for all return periods. Nonetheless, this hybrid approach is widely used by the engineering and scientific community (called Approach 1 or Approach 2 in NUREG 6728).

The procedure is similar to level 1c, with one difference: the site response is nonlinear, and the NOAH code operates in the time domain. Acceleration time series compatible with the UHS reference rock spectrum must be used. We have selected ten real accelerograms corresponding to the scenario events (Mw=[6.0-7.0] and Rhyp=[0-20] km, see Annex A), and tuned them to the VSC-KC corrected UHS spectrum using the iterative procedure used in Causse et al. (2014): the original Fourier phase spectrum of the real accelerograms is kept unchanged to capture the actual nonstationarity, while the Fourier amplitude spectrum is iteratively adapted to optimally match the target response spectrum.

The average amplification function is obtained in the Fourier domain (Figure 14d), according to (Eq. 22):

$$TF(f) = \langle FAS_{site,i}(f)/FAS_{rock,i}(f) \rangle \quad \text{Eq. 22}$$

where the symbol < > stands for the geometrical average of the Fourier spectral ratios over the selected time series *i*. The amplification obtained is significantly reduced with respect to the linear case, especially in the high frequency range. The resulting average transfer function is displayed in Figure 14d and its corresponding surface response spectrum is displayed in Figure 15b. This method predicts the lowest amplitudes among the different method implemented (up to 1.0 s). The UHS obtained is close to the UHS level 1a, relying on a residual scaling with site term (WIST), the method that accounts for non-linear behavior in a generic way.

- Full Probabilistic Integration Based Method

Cramer (2003) and Bazzuro & Cornell (2004b) were the first authors to propose and implement a method to account for site effects in a fully probabilistic framework. This method, corresponding to level 2b, is named here the Full Probabilistic Integration Based Method and is equivalent to Approach 3 in NUREG 6728. The site amplification function is convolved with the hazard on rock, as follows:

$$HC_{Soil}(Z) = \int_0^\infty P\left[Y \geq \frac{Z}{x} \middle| x\right] f_x(x)dx \quad \text{Eq. 23}$$

where HC means hazard curve, i.e. annual probability of exceedance as a function of soil hazard level $Z=S_{as(f)}$; x is rock hazard, $x=S_{ar(f)}$; Y is the input dependent site amplification $Y= AF(f, S_{ar})$ and $P(Y)$ its distribution conditioned by the rock motion level; $f_{x(x)}$ is the probability density function (*pdf*) of $S_{ar(f)}$. Most codes currently used to calculate PSHA do not include this feature. The OpenQuake engine (http://www.globalquakemodel.org/) would need to be modified to include such a tool. We did not apply this method to Euroseistest.

- Level 2c – Full Convolution Analytical Method (AM)

Bazzurro & Cornell (2004b) proposed to replace the numerical convolution process (Eq. 23) by an analytical one making use of a closed form solution. Several assumptions are required:

i. The median amplification function $AF\ (f, S_{ar})$ can be described by a piece-wise linear dependence on the rock motion Sar (in a log-log scale at every frequency);
ii. Its variability can be described by a lognormal distribution,
iii. The rock hazard can be represented locally (around the return period of interest) by a power law dependence on hazard level.

Such an approach is very appealing since it offers several advantages:

i. The amplification due to site effects is considered as an a posteriori correction to the hazard calculations.
ii. The full probabilistic meaning of the hazard curve and UHS is respected.
iii. The calculations of the hazard curve on soil are very simple and with low computational demand.

The implementation of this method in Bazzurro & Cornell (2004b) indicate that such assumptions are acceptable. Nonetheless, Aristizabal et al. (2018) have shown that for the Euroseistest site, the non-linearity is too strong at intermediate to large return periods. Some terms in the closed form solution get unrealistically large values, using either the nonlinear code NOAH or the equivalent linear SHAKE code (Schnabel 1972). This happens whenever the ground acceleration saturates because of limited strength. Aristizabal et al. (2018) have shown that the method is not adapted to soft deposits at Euroseistest.

- Level 2d – Classical PSHA with Soil Specific Attenuation Equation

Bazurro & Cornell (2004b) proposed to simply tune the GMPE used in the hazard calculation. The GMPE is turned into a site-specific GMPE by replacing its generic site term by a specific one tuned to the site-specific, non-linear numerical simulations, as follows:

$$ln\, Sa_{Soil}(f) = ln\, Sa_{RockGMPE,i}(f) + ln(AF_{Site-Specific}(f)) \quad \text{Eq. 24}$$

This approach is equivalent to approach 4 in NUREG 6728 (McGuire et al., 2001); it was applied by Papastiliou et al. (2012b). In the Euroseistest case, the reference rock is much harder than the site conditions accounted for in most GMPEs and the rock GMPE should be first corrected for rock hardness. Although this

could be achieved with the V_S-κ corrections, it was not applied here as it is not yet implemented in the OpenQuake engine, used for PSHA computations.

- Level 2e – Full Probabilistic Stochastic Method

Aristizabal et al. (2018) proposed to account for site response in PSHA in a fully probabilistic way, combining Monte Carlo sampling and time series simulations. Rather than integrating frequency-magnitude distributions as in classical PSHA, a very long earthquake catalog is generated from the source model with the Monte Carlo method. A stochastic point-source approach (Boore, 2003), that provides synthetic time histories on rock for every earthquake in the catalog, is combined with a 1D numerical site response code to propagate the time histories from depth to surface. The hazard curve is then established from simple statistics on the synthetic ground-motions at the soil surface. Two site response codes are used, an equivalent-linear (SHAKE91, Schnabel et al. 1993) and a non-linear code (NOAH, Bonilla, 2001) to illustrate the large uncertainty associated to this step.

There is one step in the method that was difficult to tackle, the tuning of the source and path parameters required by the Boore (2003) stochastic point-source approach. The synthetic hazard curve obtained on rock, directly from the exceedance rates of stochastic time histories, should fit the hazard curve on the reference rock obtained applying classical PSHA (application of GMPE Akkar et al. 2014, as well as V_S-κ corrections). More details are provided in Aristizabal et al. (2018).

The calculations were performed for three spectral periods: PGA (0s), 0.2 s and 1.0 s. For the 5,000 year return period, the resulting hazard values are 0.4, 0.45 and 0.65 g when using the linear equivalent approach (SHAKE), and 0.2, 0.65 and 0.7 g when using a fully non-linear simulation code (NOAH). These values actually correspond to the mean NL "saturation" levels provided by the extensive 1D NL site response simulations, illustrated in Figure 12 of Aristizabal et al. (2018). These results also show that the saturation is reached for input motion levels with return periods lower than 5000 years for the reference hard rock (see Figure 9). The saturation thus corresponds to the vertical asymptote of the site-surface hazard curves, and it must be emphasised that such asymptotes are extremely sensitive to the constitutive law adopted for the soft soils: The epistemic uncertainty associated to NL 1D site response is very large.

These hazard values are indeed significantly lower than those obtained with the hybrid level 2a approach (Figure 14b), although both results were obtained with the same fully NL code (NOAH). We cannot propose yet definitive explanations for this apparent inconsistency. Nevertheless, the response of NL systems is known to be highly dependent both on the frequency content of the excitation and on its phase properties. The stochastic simulations used as input in Aristizabal et al. (2018) are characterised by a random phase, while the real signals considered here are non-stationary and have non-random phase properties. We consider that these phase properties of the input motion might be the origin of the large differences, in agreement with the results by Causse et al. (2014), who find a much lower variability of NL 1D site response for random phase signals compared with real signals. When considering the NL response plots in Figure 12 of Aristizabal et al. (2018), one can notice the upper bound of the saturation levels is slightly higher than the mean values indicated above, i.e., 0.5, 0.6 and 1.0 g for SHAKE, and 0.2, 0.7 and 1.0 g for NOAH, for spectral periods PGA, 0.2 and 1.0 s, respectively. These values are also indicated with specific symbols at the corresponding spectral periods in Figure 15b.

DISCUSSION

The hazard results obtained at Euroseistest are summarised in Figure 16. The uniform hazard spectra obtained for soil following different methodologies are superimposed in Figure 16a to the uniform hazard spectra obtained for different rock references. These results have been obtained at one unique location, nonetheless their analysis leads to a few key conclusions that may be of interest for any site-specific hazard assessment.

All the analysis is based on a single GMPE (AA14), which was selected as an accepTable choice since it predicts levels that correspond to the average acceleration considering the eight models selected. Besides, the AA14 GMPE is a relatively recent GMPE with a clear separation between-event (τ) and within-event (ϕ) aleatory variability terms, which are fundamental for this study. Moreover, this GMPE was in the short list of equations selected for crustal earthquakes in the GEM project (Stewart et al., 2015). Nevertheless, an interesting exercise could be to replicate this study with other GMPEs to validate the findings, i.e. the important approach-to-approach uncertainty observed whatever the ground motion model.

The variability obtained, with the use of one single GMPE, for the UHS on rock (in grey) comes mainly from the consideration of a full or reduced aleatory variability, and from the characteristics of the reference rock (velocity and attenuation, within or outcropping motion conditions). At 0.1s, the amplitude varies between 0.8 and 1.5g. The variability obtained on soil, including the soft soil response, is significantly enlarged, e.g. the amplitude varies between 1.1 and 4.0 g at 0.1s. This increase of the hazard variability on soil with respect to rock was observed after applying the generic PSHA approach with different GMPEs (level 0a, see Section 6.1.1. While the variability on rock is mostly related to the reference rock properties (shear-wave velocity, kappa, outcropping or within motion), the variability on soil is also related to the selected method to derive the site-specific hazard (method-to-method variability).

This study provides some hints on the main elements controlling the variability of hazard estimates at the soil surface (Figure 16b). The most striking one is the type of soil behavior, linear or non-linear. As expected, the linear approaches predict systematically larger hazard values (in magenta) than methods that consider nonlinear behavior (in green), especially at short periods. The difference in the results between linear and nonlinear methods is particularly exacerbated at Euroseistest because of the presence of very soft soils at shallow depth, and of a thick alluvial deposit with a large impedance contrast at large depth. For large input motion, shear strains reach large values over the whole soil column, result-

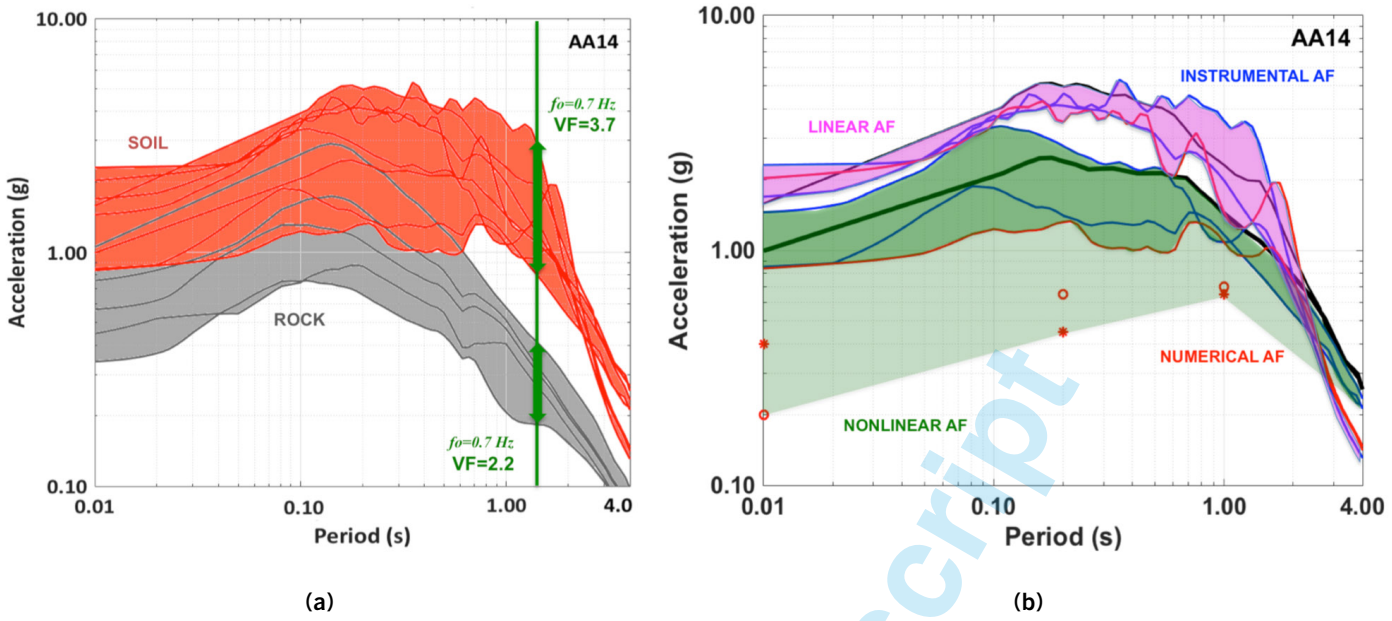

Fig. 16 - Summary of uniform hazard spectra (5000 years return period) obtained at Euroseistest (TST location): (a) Distribution of UHS obtained on rock (grey) and on soil (red) with various generic, partially and fully site-specific approaches (levels 0a, 0b, 1a, 1b, 1c and 2a, see Table 7); (b) UHS obtained at the surface on soft soil, distinguishing linear (magenta) and nonlinear (green) approaches, instrumental (blue) and numerical (red) estimates. The strong green area stand for the NL results presented in this study, the light green extension includes the results of Aristizabal et al., 2018b. The UHS obtained with a generic approach (level 0) using AA14 GMPE for V_{S30}=186 m/s is also superimposed (black).

ing in significant to large damping, which "kills" the reverberation phenomena and the associated resonances.

At the Euroseistest TST station, the hazard estimates accounting for nonlinearity are thus much lower than hazard estimates relying on linear amplification. Such reduction of hazard might be expected for most sites with thick and soft deposits in highly active seismic areas. The consideration of linear amplification could be appropriate for short return periods in seismic zones with moderate to low activity. Nevertheless, for large return periods (or even for intermediate return periods in highly seismic zones such as at Euroseistest), ignoring nonlinearity leads to an overestimation of the hazard, with unrealistic high levels. Site-specific studies accounting for nonlinear site response is thus highly recommended. In most cases, nonlinearity can be evaluated with numerical simulations only as there are very few sites with a large enough number of strong events recordings. The uncertainty related to the choice of the non-linear code needs to be addressed. The recent benchmarking exercises on nonlinear simulation codes (e.g., Stewart et al., 2008, Régnier et al., 2016b, 2018) have demonstrated that the numerical estimates of nonlinear site response are associated with a significant amount of epistemic uncertainty, which increases with the input motion level. We did not consider this particular kind of epistemic uncertainties in the present study.

The results show that the 1D numerical linear amplification function (red line in magenta zone, Figure 16b) underestimates the hazard estimates obtained with linear instrumental functions. It strongly suggests that 2D/3D effects are present and significant, as shown in Maufroy et al. (2016, 2017), and that they do impact the instrumental data but cannot be captured with a simple 1D wave propagation model. 2D/3D simulation tools, or at least 2D/3D aggravation factors (Riga et al., 2016; Boudghene-Stambouli et al., 2018; Kristek et al., 2018; Moczo et al., 2018) should be used to derive more realistic estimates of AF(f). They have not been considered here to avoid too many complexities, but their results would probably be similar to those obtained with instrumental estimates of AF(f). Even though such basin effects are certainly affected by soil non-linearity, they might remain significant at least at low frequencies, where damping effects are less important and 1D non-linear simulations considered in level 2 approaches may have an underestimation bias. 2D/3D non-linear simulation codes do exist and are used by several groups and companies, but one must keep in mind that they have never been cross-checked by any benchmarking exercise, and that it is likely that the associated model uncertainty is higher than the one associated to 1D nonlinear codes (see Régnier et al., 2016, 2018). A simple solution on the safe side would be to apply the linear 2D/1D or 3D/1D aggravation factors (Moczo et al., 2018) to the results of 1D nonlinear numerical simulation.

Amongst the generic approaches, the level 0b approaches using site terms based on more than one proxy (here f_0 and V_{S30} proxies,) lead to a significantly larger hazard than if considering only the V_{S30} proxy in the GMPE (level 0a, see Figure 12b and Figure 15a). The SAPE does not account for nonlinear behavior, while the selected GMPE does account for it in a generic way (especially in the short period range). The cumulated effects of low values of both f_0 and V_{S30} proxies lead to larger (linear) amplification in the SAPE case than the sole effect of a low V_{S30} considered in most GMPEs (including AA14). This explains the differences at long periods, where moreover nonlinear effects are not expected to be significant. It is therefore recommended to develop other multi-proxy SAPEs including non-linear terms, such as for instance in Régnier et al. (2016a) or Derras et al. (2020).

The approaches using site residuals may lead to very different results depending on the way the site residuals are computed, i.e., whether the GMPE site terms are considered or not (WIST or WOST). Such differences reach factors up to 3 (see Figure 14a) with the AA14 GMPE, and come primarily from the non-linear site term in AA14. The $\delta S2Ss$ residuals are estimated mainly from weak to moderate motion recordings, and thus correspond to linear site response residuals. When they are estimated with respect to rock motion, their application to much stronger motion does not take into account the changes in site response due to non-linear behavior. Conversely, when they are estimated with respect to the "generic site" motion, their application to much stronger motion combines the linear, site-specific part, and the non-linear, generic site term embedded in the GMPE. The impact of non-linearity for the present thick, soft site is so large that the WIST approach considering full sigma leads to much lower hazard than for the WOST approach considering single-station sigma.

Our aim is to understand the impact of some methodological choices on the hazard estimates, we did not perform a complete hazard study for the Euroseistest site. A complete hazard study would require the consideration of several GMPEs, with the associated GMPE-specific HTT adjustments, and the consideration of the epistemic uncertainty associated to each site amplification AF(f), for each site-specific approach. For instance, numerical estimates of AF(*f*) (or transfer function TF(f)) should include the variability associated to uncertainties in soil characteristics (velocity and damping profiles, non-linear properties), and to simulation codes as well (1D-2D-3D, various implementations of nonlinear behavior, which were shown to imply an uncertainty factor of at least a factor ± 50% during the PRENOLIN Benchmark, Régnier et al., 2016b, 2018). Instrumental estimates of AF(*f*) or TF(f) derived from any accepTable technique (site-to-reference spectral ratio, site residual, generalised inversion, etc.) should also include the event-to-event variability. Most probabilistic hazard software do not yet include all the corresponding tools, so that it should be performed through dedicated, post-processing codes. Nevertheless, we consider that a proper accounting for these additional epistemic uncertainties would not drastically modify the approach-to-approach variability that is obtained in this study.

LESSONS FOR SITE-SPECIFIC HAZARD STUDIES

Site-specific hazard calculations aim to provide improved hazard estimates at well-characterised sites. The differences between the "generic" site terms included in state-of-the art GMPEs and site-specific site response may have different physical origins, related to the poor characterization of a site with a single proxy (most often the "shallow" parameter V_{S30}). A single proxy cannot simultaneously properly account for 2D or 3D geometrical effects, the impedance contrast with the local deep bedrock, and the non-linear properties of the site material. Moreover, the site-specific estimates of site response and the hazard on rock can be decoupled only if the site-response is linear and without any dependence on source characteristics (e.g., azimuth or depth). At present, there is an overall consensus in the engineering community to neglect source characteristics, but to account as much as possible for soil non-linearity. As only the most recent GMPEs are able to take into account nonlinear behavior, and only in a very generic and approximate way, classical PSHA methods and software are not presently designed to provide site-specific hazard estimates in a fully satisfactory way.

Several approaches have been proposed over the last two decades to combine rock-hazard with site-specific estimates of site response, with different complexity levels and different sources of epistemic uncertainty. The aim of this work was to illustrate the application of various approaches on one example site, discuss the associated issues, and compare their results, in order to better appreciate the "benefits" versus the required costs and efforts when performing this type of analysis.

There are certainly numerous limitations in this single example of application, which prevent from drawing too general conclusions and recommendations. The example site is characterised by a large amplification over a broad frequency range, due to a combination of several factors (the large velocity contrast at depth, the low velocity at surface, and the graben structure leading to additional "basin effects"). As a consequence, the true site amplification is significantly larger than the generic, average amplification accounted for in GMPEs. The site-specific hazard estimates are larger than the generic level 0a estimates for low acceleration levels / short return periods. On the contrary, the site-specific hazard estimates are lower than the generic estimates at long return periods / large acceleration levels, due to the softness and thickness of the alluvial deposits, associated to a large impedance contrast, that exacerbates the impact of non-linear effects. We derive the following "lessons" for sites similar to the Euroseistest TST site, but we consider that some of these lessons might be valid for other types of soil sites.

From a purely scientific viewpoint, there is no doubt that a site-specific approach is always preferable, whatever it costs, as it is based on a refined knowledge of the site characteristics and the site response. However, site-specific hazard studies are most often targeted on critical industrial facilities. The owners of these facilities have to decide whether they take on the associated additional cost with respect to a "classical" generic (level 0a) study. The arguments most often put forward to rationalise such an additional cost are, on the scientific side, the avoidance of a double-counting of uncertainty and an improvement in the mean estimate of hazard at the site, and sometimes also on the economic side with the possibility of some hazard reduction due to the use of single-station standard deviation (σ_{ss}) instead of the ergodic one (σ). The latter argument does not prove to be verified in the present Euroseistest example, although it is one of the best-known sites worldwide. The amount of additional epistemic uncertainties associated with the various site-specific approaches compensate the reduction of aleatory uncertainty, for all cases but level 2 approaches that take into account site non-linearities. In level 2 approaches, the joint consideration of single-site sigma and nonlinear site response, or the consideration of full sigma with the "WIST" site residual approach (Level 1a), lead to a reduced hazard with respect to the level 0 approach. Moreover, the drastic hazard reduction due to nonlinear effects should not be generalised to all possible real situations, since the present example corresponds to a rather highly active seismic area, with thick and soft-soils with high impedance contrast at large

depth, implying a large strains over a large depth and prominent damping effects. We believe that scientists should not promise a systematic reduction in hazard estimates with site-specific studies.

In parallel to fully site-specific studies, it is thus probably reasonable to develop some intermediate-complexity approaches. A promising approach is the development of "stand-alone" SAPEs, which could be added independently to any "rock" GMPE. The joint use of multiple site proxies and neural network tools (see for instance the recent overview by Bergamo et al., 2020) may allow to provide statistical, still generic, predictions of site response that are closer to the actual one, and may also include non-linear (Derras et al., 2020) or geometrical effects (Boudghene-Stambouli et al., 2018). Another recommended approach is to equip the site under study with sensitive, instrumentation: even in moderately active areas, a few years at most are enough to obtain enough recordings to apply the level 1a approach: the coupling between site-specific residuals (linear domain) and generic, non-linear terms embedded in the GMPEs does bring significant improvement with respect to the fully generic GMPE approach.

Of course, improvements are also needed concerning fully site-specific approaches. From a methodological viewpoint, considering the prominent effects of soil non-linearity and 2D/3D effects in the Euroseistest case, high priority should be given to the development of numerical simulation codes coupling 2D/3D effects and non-linear behavior, and to their careful benchmarking through verification and validation exercise similar to what has been recently achieved on 1D simulation tools (Stewart et al., 2008; Régnier et al., 2016b, 2018). As also mentioned earlier, site-specific hazard studies should also include the consideration of epistemic uncertainties in site response estimates. Some of these uncertainties, especially when considering 2D and 3D effects, are related to the sensitivity of site response to the back-azimuth and incidence angles of incoming waves, as shown in Maufroy et al. (2017) for the Euroseistest case. Methodological developments coupling this sensitivity with a disaggregation of rock hazard could be one way to limit the impact of such epistemic uncertainties on the increase of hazard estimates.

In summary, site-specific hazard estimates for sites with complex geometry and rheology, face difficulties related to large epistemic uncertainties and approach-to-approach variability. These large epistemic uncertainties can lead to an increase of hazard estimates, counterbalancing the decrease due to the use of reduced sigma in GMPEs. Such a result might suggest that uncertainties in generic hazard estimates are likely to be underestimated.

ACKNOWLEDGEMENTS

This work has been supported by a grant from Labex OSUG@2020 (Investissements d'avenir –ANR10 LABX56 - http://www.osug.fr/labex-osug-2020/) and by the European STREST project (Harmonised approach to stress tests for critical infrastructures against natural hazards - http://www.strest-eu.org). Special thanks are due to Fabian Bonilla for facilitating the use of the nonlinear code NOAH (Bonilla, 2000) and additional technical assistance on its usage. Also, we would like to acknowledge Olga J. Ktenidou and Fabrice Cotton for providing the site-specific residuals analysis at the Euroseistest, as well as to Fabrice Hollender and Nikos Theodoulidis for facilitating valuable geotechnical and site-specific data to build the nonlinear models. All ground-motion records used in this study were downloaded using the PEER Strong-motion Database (Pacific Earthquake Engineering Research Center - http://ngawest2.berkeley.edu/). Hazard calculations on rock and soil (only Level 0) have been performed using the Openquake engine and the post-processing toolkits developed by the GEM Foundation (http://www.globalquakemodel.org/), as well as the SHARE area source model (http://www.share-eu.org/). The software Strata developed by Albert Kottke was used to perform the IRVT and RVT calculation and is publicly available at (https://github.com/arkottke/irvt/).

REFERENCES

Abrahamson N.A. (2012) - Application of Single-Station Sigma Ground-motion Prediction Equations in Practice. 15th World Conference on Earthquake Engineering, (WCEE), September 24-28, 2012, Lisbon, Portugal.

Abrahamson N.A. & Sykora D. (1993) - Variations of ground-motions across individual sites. In Proc. of the DOE Natural Phenomena Hazards Mitigation Conf (pp. 192-198).

Abrahamson N. A., Kuehn N. M., Walling M. & Landwehr N. (2019). Probabilistic seismic hazard analysis in California using nonergodic ground-motion models. Bulletin of the Seismological Society of America, 109(4), 1235-1249.

Akkar S. & Bommer J.J. (2010) - Empirical equations for the prediction of PGA, PGV, and spectral accelerations in Europe, the Mediterranean region, and the Middle East. Seismological Research Letters, 81(2), 195-206, https://doi.org/10.1785/gssrl.81.2.195.

Akkar S., Sandıkkaya M.A., Bommer J. J. et al., (2014) - Empirical Ground-motion Models for Point- and Extended-Source Crustal Earthquake Scenarios in Europe and the Middle East. Bulletin of Earthquake Engineering, 12(1), 359-387.

Atik L.A., Abrahamson N., Bommer J.J., Scherbaum F., Cotton F. & Kuehn N. (2010) - The variability of ground-motion prediction models and its components. Seismological Research Letters, 81(5), 794-801.

Al Atik L., Kottke A., Abrahamson N. & Hollenback J. (2014) - Kappa (κ) scaling of ground-motion prediction equations using an inverse random vibration theory approach. Bulletin of the Seismological Society of America, 104(1), 336-346, https://doi.org/10.1785/0120120200.

Anderson J.G. & Hough S. E. (1984) - A model for the shape of the Fourier amplitude spectrum of acceleration at high frequencies. Bulletin of the Seismological Society of America, 74(5), 1969-1993.

Andrews D. J. (1986) - Objective determination of source parameters and similarity of earthquakes of different size. In: S. Das, J. Boatwright, and C. H. Scholz (Eds), Earthquake Source Mechanics, American Geophysical Union, Washington, D.C., 259-268.

Aristizábal C., Bard P.Y., Beauval C., Lorito S. & Selva J. (2016) - Guidelines and case studies of site monitoring to reduce the uncertainties affecting site-specific earthquake hazard assessment. STREST Deliverable D3.4 - Harmonized approach to stress tests for critical infrastructures against natural hazards (http://www.strest-eu.org/opencms/opencms/results/), 2016. Web. 25 Apr. 2016.

Aristizabal C. (2018a) - Integration of site effects into probabilistic seismic hazard methods (Doctoral dissertation, Université Grenoble Alpes).

Aristizabal C., Bard P.-Y., Beauval C. & Gómez J.C (2018b) - Integration of Site Effects into Probabilistic Seismic Hazard Assessment (PSHA): A Comparison between Two Fully Probabilistic Methods on the Euroseistest Site. Geosciences, 8, 285.

Barani S. & Spallarossa D. (2017) - Soil amplification in probabilistic ground motion hazard analysis. Bulletin of Earthquake Engineering, 15(6), 2525-2545.

Bard P.Y., Bora S.S., Hollender F., Laurendeau A. & Traversa P. (2020) - Are the standard VS-Kappa host-to-target adjustments the only way to get consistent hard-rock ground motion prediction? Pure and Applied Geophysics, 177(5), 2049-2068, https://doi.org/10.1007/s00024-019-02173-9

Bazzurro P. (1998) - Probabilistic seismic damage analysis, Ph.D. Dissertation, Stanford University, Stanford, California.

Bazzurro P. & Cornell C.A. (2004a) - Ground-motion Amplification in Nonlinear Soil Sites with Uncertain Properties. Bulletin of the Seismological Society of America, 94(6), 2090-2109, December 2004.

Bazzurro P. & Cornell C.A. (2004b) - Nonlinear Soil-Site Effects in Probabilistic Seismic-Hazard Analysis Bulletin of the Seismological Society of America, 94(6), 2110-2123, December 2004.

Bergamo P., Hammer C. & Fäh D. (2020) - Towards improvement of site condition indicators. Deliverable 7.4 of Work package WP7 Networking databases of site and station characterization, SERA EU Project (Seismology and Earthquake Engineering Research Infrastructure Alliance for Europe; Horizon 2020, grant agreement #730900). http://www.sera-eu.org/export/sites/sera/home/.galleries/Deliverables/SERA_D7.4_IMPROVEMENT_SITE_INDICATORS-1.pdf

Bergamo P., Hammer C. & Fäh D. (2021) - On the relation between empirical amplification and proxies measured at Swiss and Japanese stations: Systematic regression analysis and neural network prediction of amplification. Bulletin of the Seismological Society of America, 111(1), 101-120.

Bonilla L.F. (2000) - NOAH: User's Manual, Institute for Crustal Studies, University of California, Santa Barbara.

Boore D. (2003) - Simulation of ground-motion using the stochastic method. Pure and Applied Geophysics, 160(3-4), 635-676.

Boore D.M. & Joyner W.B. (1997) - Site amplifications for Generic Rock Sites, Bull. Seismol. Soc. Am., 87, 327-341.

Boore D.M., Stewart J.P., Seyhan E. & Atkinson G.M. (2014) - NGA-West2 equations for predicting PGA, PGV, and 5% damped PSA for shallow crustal earthquakes. Earthquake Spectra, 30(3), 1057-1085.

Bozorgnia Y., Abrahamson N.A., Atik L.A., Ancheta T.D., Atkinson G.M., Baker J.W., Baltay A., Boore D.M., Campbell K.W., Chiou B.S.-J., Darragh R., Day S., Donahue J., Graves R.W., Gregor N., Hanks T., Idriss I.M., Kamai R., Kishida T., Kottke A., Mahin S.A., Rezaeian S., Rowshandel B., Seyhan E., Shahi S., Shantz T., Silva W., Spudich P., Stewart J.P., Watson-Lamprey J., Wooddell K. & Youngs R. (2014) - NGA-West2 research project. Earthquake Spectra, 30(3), 973-987.

Boudghene-Stambouli A.B., Zendagui D., Bard P.-Y. & Derras B. (2017) - Deriving amplification factors from simple site parameters using generalized regression neural networks: implications for relevant site proxies. Earth, Planets and Space, 69(1), 99.

Boudghene-Stambouli A., Bard P.-Y., Chaljub E., Moczo P., Kristek J., Stripajova S., Durand C., Zendagui D. & Derras B. (2018) - 2D/1D Aggravation Factors: From A Comprehensive Parameter Study To Simple Estimates With A Neural Network Model. 16ECEE (16th European Conference on Earthquake Engineering), Thessaloniki, Greece, June 18-21, 2018, paper #624, 12 pages.

Cadet H., Bard P.-Y. & Rodriguez-Marek A. (2012a) - Site effect assessment using KiK-net data: Part 1. A simple correction procedure for surface/downhole spectral ratios, Bulletin of Earthquake Engineering, 10(2), 421-448.

Cadet H., Bard P.-Y., Duval A.-M. & Bertrand E. (2012b) - Site effect assessment using KiK-net data: part 2. Site amplification prediction equation based on f_0 and V_{sz}., Bulletin of Earthquake Engineering 10(2), 451-489.

Campbell K.W. (2003) - Prediction of strong ground motion using the hybrid empirical method and its use in the development of ground-motion (attenuation) relations in eastern North America. Bulletin of the Seismological Society of America, 93(3), 1012-1033.

Causse M., Laurendeau A., Perrault M., Douglas J., Bonilla F. & Guéguen P. (2014) - Eurocode 8-compatible synthetic time-series as input to dynamic analysis. Bulletin of earthquake engineering, 12(2), 755-768. https://doi.org/10.1007/s10518-013-9544-2.

Cauzzi C., Edwards B., Donat F., Clinton J., Wiemer S., Kästli P., Cua G., Giardini D. (2014) - New predictive equations and site amplification estimates for the next-generation Swiss ShakeMaps. Geophysical Journal International, 200(1), 421-438. https://doi.org/10.1093/gji/ggu404.

Cauzzi C., Faccioli E. & Costa G. (2008) - Broadband (0.05 to 20 s) prediction of displacement response spectra based on worldwide digital records. Journal of Seismology, 12(4), 453-475.

Çelebi M., Sahakian V. J., Melgar D., & Quintanar L. (2018) - The 19 September 2017 M 7.1 Puebla-Morelos earthquake: Spectral ratios confirm Mexico City zoning. Bulletin of the Seismological Society of America, 108(6), 3289-3299.

Chaljub E., Maufroy E., Moczo P., Kristek J., Hollender F., Bard P.-Y., Priolo E., Klin P., de Martin F., Zhang Z., Zhang W. & Chen X. (2015) - 3-D numerical simulations of earthquake ground-motion in sedimentary basins: testing accuracy through stringent models. Geophysical Journal International, 201(1), 90-111.

Chávez-García F.J. & Bard P.-Y. (1994) - Site effects in Mexico City eight years after the September 1985 Michoacan earthquakes. Soil Dynamics and Earthquake Engineering, 13(4), 229-247.

Chávez-García F.J., Raptakis D., Makra, K. & Pitilakis K. (2000) - Site effects at Euroseistest—II. Results from 2D numerical modeling and comparison with observations. Soil Dynamics and Earthquake Engineering. 19(1), 23-39. https://doi.org/10.1016/S0267-7261(99)00026-3.

Chávez-García F.J. & Faccioli E. (2000) - Complex site effects and building codes: Making the leap. Journal of Seismology, 4, 23-40. Kluwer Academic Publishers.

Chiou B. S.-J. & Youngs R.R. (2008) - An NGA model for the average horizontal component of peak ground-motion and response spectra. Earthquake Spectra, 24(1), 173-215.

Chiou B. S.-J. & Youngs R.R. (2014) - Up-date of the Chiou and Youngs NGA model for the average horizontal component of peak ground motion and response spectra. Earthquake Spectra 30, 1117-1153.

Cotton F., Scherbaum F., Bommer J.J. & Bungum H. (2006) - Criteria for selecting and adjusting ground-motion models for specific target regions: Application to central Europe and rock sites. Journal of Seismology, 10(2), 137-156, https://doi.org/10.1007/s10950-005-9006-7.

Cramer C.H. (2003) - Site-specific seismic-hazard analysis that is completely probabilistic. Bulletin of the Seismological Society of America, 93(4), 1841-1846.

Delavaud E., Scherbaum F., Kuehn N. & Allen T. (2012) - Testing the global applicability of ground-motion prediction equations for active shallow crustal regions. Bulletin of the Seismological Society of America, 102(2), 707-721, https://doi.org/10.1785/0120110113.

Derras B., Bard P.-Y. & Cotton F. (2016) - Site-Condition Proxies, Ground-motion Variability, and Data-Driven GMPEs: Insights from the NGA-West2 and RESORCE Data Sets. Earthquake spectra, 32(4), 2027-2056.

Derras B., Bard P.-Y., Régnier J. & Cadet H. (2020) - Non-linear modulation of site response: Sensitivity to various surface ground-motion intensity measures and site-condition proxies using a neural network approach. Engineering Geology, 269, https://doi.org/10.1016/j.enggeo.2020.105500.

Douglas J., Akkar S., Ameri G., Bard P.-Y., Bindi D., Bommer J.J., Singh Bora S., Cotton F., Derras B., Hermkes M., Kuehn N. M., Luzi L., Massa M., Pacor F., Riggelsen C., Sandıkkaya M.A., Scherbaum F., Stafford P.J. & Traversa P. (2014) - Comparisons among the five ground-motion models developed using RESORCE for the prediction of response spectral accelerations due to earthquakes in Europe and the Middle East. Bull. Earthquake Eng., 12(1), 341-358, https://doi.org/10.1007/s10518-013-9522.

Galvis F., Miranda E., Heresi P., Dávalos H. & Silos J. R. (2017) - Preliminary Statistics of Collapsed Buildings in Mexico City in the September 19, 2017 Puebla-Morelos Earthquake. John A. Blume Earthq. Engineering. Ctr., Stanford University.

Haji-Soltani A. & Pezeshk S. (2017) - A Comparison of Different Approaches to Incorporate Site Effects into PSHA: A Case Study for a Liquefied Natural Gas TankA Comparison of Different Approaches to Incorporate Site Effects into PSHA: A Case Study for an LNG Tank. Bulletin of the Seismological Society of America, 107(6), 2927-2947.

Jongmans D., Pitilakis K., Demanet D., Raptakis D., Riepl J., Horrent C., Tsokas G., Lontzetidis K. & Bard P. Y. (1998) - EURO-SEISTEST: determination of the geological structure of the Volvi basin and validation of the basin response. Bulletin of the Seismological Society of America, 88(2), 473-487. https://doi.org/10.1785/BSSA0880020473

Konno K. & Ohmachi T. (1998) - Ground-motion characteristics estimated from spectral ratio between horizontal and vertical components of microtremor. Bulletin of the Seismological Society of America, 88(1), 228-241.

Kotha S.R., Weatherill G., Bindi D. & Cotton F. (2020) - A regionally-adapTable ground-motion model for shallow crustal earthquakes in Europe. Bulletin of Earthquake Engineering, 18, 4091-4125

Kottke A.R. & Rathje E.M. (2008a) - Technical Manual for Strata. PEER Report 2008/10. University of California, Berkeley, California.

Kottke A.R. & Rathje E.M. (2008b) - A Semi-Automated Procedure for Selection and Scaling of Recorded Earthquake Motions for Dynamic Analysis. Earthquake Spectra, Earthquake Engineering Research Institute, 24(4), 911-932.

Kottke A.R. (2017) - VS30–κ0 relationship implied by ground-motion models? In 16th World Conference on Earthquake Engineering (16WCEE).

Kramer S. L. (1996) - Geotechnical Earthquake Engineering. Prentice-Hall, Inc. New Jersey, 348-422.

Kristek J., Moczo P., Bard P.-Y., Hollender F. & Stripajová S. (2018) - Computation of amplification factor of earthquake ground motion for a local sedimentary structure, Bulletin of Earthquake Engineering, 16 (6), 2451–2475, https://doi.org/10.1007/s10518-018-0358-0.

Ktenidou O.J., Cotton F., Abrahamson N.A. & Anderson J.G. (2014) - Taxonomy of κ: A review of definitions and estimation approaches targeted to applications. Seismological Research Letters, 85(1), 135-146.

Ktenidou O.J., Roumelioti Z., Abrahamson N.A., Cotton F., Pitilakis K. & Hollender F. (2015a) - Site effects and ground-motion variability: traditional spectral ratios vs. GMPE residuals. SSA Annual Meeting, Pasadena, 21-23 April.

Ktenidou O.J., Abrahamson N.A., Drouet S. & Cotton F. (2015b) - Understanding the physics of kappa (κ): Insights from a downhole array. Geophysical Journal International, 203(1), 678-691.

Ktenidou O.J., Roumelioti Z., Abrahamson N.A., Cotton F., Pitilakis K. & Hollender F. (2018) - Understanding single-station ground motion variability and uncertainty (sigma): lessons learnt from EUROSEISTEST. Bulletin of Earthquake Engineering, 16(6), 2311-2336.

Laurendeau A., Foundotos L., Hollender F. et al., (2015) - Correction of surface records of their site effect before developing GMPE: an alternative approach to get reference incident ground-motion (application to KiK-net data). Sigma / SINAPS@ deliverable SINAPS@-2015-V1-A1-T3-1, 74 pages.

Laurendeau A., Bard P.-Y., Hollender F., Perron V., Foundotos L., Ktenidou O.J. & Hernandez B. (2018) - Derivation of consistent hard rock (1000< V S< 3000 m/s) GMPEs from surface and down-hole recordings: analysis of KiK-net data. Bulletin of Earthquake Engineering, 16(6), 2253-2284. https://doi.org/10.1007/s10518-017-0142-6.

Lee R.C. (2000) - A methodology to integrate site response into probabilistic seismic hazard analysis, Site Geotechnical Services, Savannah River Site, 3 February 2000.

Lee R.C., Maryak M. E. & Kimball J. (1999) - A methodology to estimate site-specific seismic hazard for critical facilities on soil or soft-rock sites (abstract), Seism. Res. Lett., 70, 230.

Lee R.C., Silva W.J. & Cornell C.A. (1998) - Alternatives in evaluating soil- and rock-site seismic hazard (abstract), Seism. Res. Lett., 69, 81.

Luzi L., Puglia R., Pacor F., Gallipoli M.R. et al., (2011) - Proposal for a soil classification based on parameters alternative or complementary to Vs30. Bulletin of Earthquake Engineering, 9(6), 1877-1898.

Makra K. & Chávez-García F.J. (2016) - Site effects in 3D basins using 1D and 2D models: an evaluation of the differences based on simulations of the seismic response of Euroseistest. Bulletin of Earthquake Engineering, 14(4), 1177-1194.

Maufroy E., Chaljub E., Hollender F., Kristek J., Moczo P., Klin P., Priolo E., Iwaki A., Iwata T., Etienne V., De Martin F., Theodoulidis N., Manakou M., Guyonnet-Benaize C., Pitilakis K. & Bard P.-Y. (2015) - Earthquake ground motion in the Mygdonian basin, Greece: the E2VP verification and validation of 3D numerical simulation up to 4 Hz, Bull. seism. Soc. Am., 105, 1398-1418, https://doi.org/10.1785/0120140228.

Maufroy E., Chaljub E., Hollender F., Bard P.-Y., Kristek J., Moczo P., De Martin F., Theodoulidis N., Manakou M., Guyonnet-Benaize C., Hollard N. & Pitilakis K. (2016) - 3D Numerical simulation and ground motion prediction: Verification, validation and beyond - lessons from the E2VP project, Soil Dynamics and Earthquake Engineering 91, 53-71 (special 6ICEGE issue), http://dx.doi.org/10.1016/j.soildyn.2016.09.047.

Maufroy E., Chaljub E., Theodoulidis N., Roumelioti Z., Hollender F., Bard P.-Y., De Martin F., Guyonnet-Benaize C. & Margerin L. (2017) - Source-related variability of site response in the Mygdonian basin (Greece) from accelerometric recordings and 3-D numerical simulations. Bulletin of the Seismological Society of America, 107(2), 787-808. https://doi.org/10.1785/0120160107.

McGuire R.K., Silva W.J. & Costantino C.J. (2001) - Technical Basis for Revision of Regulatory Guidance on Design Ground-motions: Hazard- and Risk-Consistent Ground-motion Spectra Guidelines. NUREG/CR-6728, U.S. Nuclear Regulatory Commission, Washington, D.C.

McGuire R.K. & Toro G.R. (2008) - Site-specific seismic hazard analysis. 14th WCEE (World Conference on Earthquake Engineering), October 12-17, 2008, Beijing, China.

McGuire R.K., Silva W.J. & Costantino C.J. (2001) - NUREG/CR-6728. Technical Basis for Revision of Regulatory Guidance on Design Ground-motions: Hazard-and Risk-Consistent Ground Motion Spectra Guidelines. US: United States Nuclear Regulatory Commission.

Moczo P., Kristek J., Bard P.-Y., Stripajová S., Hollender F., Chovanová Z., Kristeková M. & Sicilia D. (2018) - Key structural parameters affecting earthquake ground motion in 2D and 3D sedimentary structures, Bulletin of Earthquake Engineering, 16(6), 2421-2450, https://doi.org/10.1007/s10518-018-0345-5.

Pagani M., Monelli D., Weatherill G., Danciu L., Crowley H., Silva V., Henshaw P., Butler L., Nastasi M., Panzeri L., Simionato M. & Vigano D. (2014) - OpenQuake engine: an open hazard (and risk) software for the global earthquake model. Seismological Research Letters, 85(3), 692-702.

Papastiliou M., Kontoe S. & Bommer J.J. (2012a) - An exploration of incorporating site response into PSHA - Part I: Issues related to site response analysis methods, Soil Dynamics and Earthquake Engineering, 42, 302-315.

Papastiliou M., Kontoe S. & Bommer J.J. (2012b) - An exploration of incorporating site response in to PSHA – part II: Sensitivity of hazard estimates to site response approaches, Soil Dynamics and Earthquake Engineering, 42, 316-330.

Pecker A., Faccioli E., Gurpinar A., Martin C. & Renault P. (2017) - An overview of the SIGMA research project. Springer, Berlin, https://doi.org/10.1007/978-3-319-58154-5.

Pitilakis K., Roumelioti Z., Raptakis D., Manakou M., Liakakis K., Anastasiadis A. & Pitilakis, D. (2013) - The Euroseistest strong ground-motion database and web portal. Seismological Research Letters, 84(5), 796-804, https://doi.org/10.1785/0220130030.

Pitilakis K., Raptakis D., Lontzetidis K., Tika-Vassilikou T. & Jongmans D. (1999) - Geotechnical and geophysical description of EURO-SEISTEST, using field, laboratory tests and moderate strong motion recordings. Journal of Earthquake Engineering, 3(03), 381-409.

Raptakis D., Chávez-Garcıa F. J., Makra K. & Pitilakis K. (2000) - Site effects at Euroseistest—I. Determination of the valley structure and confrontation of observations with 1D analysis. Soil Dynamics and Earthquake Engineering, 19(1), 23-39, https://doi.org/10.1016/S0267-7261(99)00026-3.

Raptakis D., Theodulidis N. & Pitilakis K. (1998) - Data Analysis of the Euroseistest Strong-motion Array in Volvi (Greece): Standard and Horizontal-to-Vertical Spectral Ratio Techniques. Earthquake Spectra, 14(1), 203-224.

Rathje E.M., Kottke A.R. & Ozbey M.C. (2005) - Using inverse random vibration theory to develop input Fourier amplitude spectra for use in site response. In Proceedings of the 16th International Conference on Soil Mechanics and Geotechnical Engineering: TC4 Earthquake Geotechnical Engineering Satellite Conference (pp. 12-16).

Rathje E.M. & Ozbey M.C. (2006) - Site-specific validation of random vibration theory-based seismic site response analysis. Journal of geotechnical and geoenvironmental engineering, 132(7), 911-922.

Rathje E.M., Pehlivan M., Gilbert M. & Rodriguez-Marek A. (2015) - Incorporating site response into seismic hazard assessment for critical facilities: a probabilistic approach. In “Perspectives on Earthquake Geotechnical Engineering”, 93-11, Springer.

Régnier J., Cadet H. & Bard P.-Y. (2016a) - Empirical Quantification of the Impact of Nonlinear Soil Behavior on Site Response. Bulletin of the Seismological Society of America, 106(4), 1710-1719, https://doi.org/10.1785/0120150199.

Régnier J., Bonilla L.F., Bard P.Y., Bertrand E., Hollender F., Kawase H., Sicilia D., Arduino P., Amorosi A., Asimaki D., Boldini D., Chen L., Chiaradonna A., DeMartin F., Ebrille M., Elgamal A., Falcone G., Foerster E., Foti S., Garini E., Gazetas G., Gélis C., Ghofrani A., Giannakou A., Gingery J.R., Glinsky N., Harmon J., Hashash Y., Iai S., Jeremić B., Kramer S., Kontoe S., Kristek J., Lanzo G., di Lernia A., Lopez-Caballero F., Marot M., McAllister G., Mercerat E.D., Moczo P., Montoya-Noguera S., Musgrove M., Nieto-Ferro A., Pagliaroli A., Pisanò F., Richterova A., Sajana S., Santisi d’Avila M.P., Shi J., Silvestri F., Taiebat M., Tropeano G., Verrucci L. & Watanabe K. (2016) - International benchmark on numerical simulations for 1D, nonlinear site response (PRENOLIN): Verification phase based on canonical cases. Bulletin of the Seismological Society of America, 106(5), 2112-2135, https://doi.org/10.1785/0120150284.

Régnier J., Bonilla L.F., Bard P.Y., Bertrand E., Hollender F., Kawase H., Sicilia D., Arduino P., Amorosi A., Asimaki D., Boldini D., Chen L., Chiaradonna A., DeMartin F., Elgamal A., Falcone G., Foerster E., Foti S., Garini E., Gazetas G., Gélis C., Ghofrani A., Giannakou A., Gingery J., Glinsky N., Harmon J., Hashash Y., Iai S., Kramer S., Kontoe S., Kristek J., Lanzo G., di Lernia A., Lopez-Caballero F., Marot M., McAllister G., Mercerat E.D., Moczo P., Montoya-Noguera S., Musgrove M., Nieto-Ferro A., Pagliaroli A., Passeri F., Richterova A., Sajana S., Santisi d’Avila M.P., Shi J., Silvestri F., Taiebat M., Tropeano G., Vandeputte D. & Verrucci L. (2018). PRENOLIN: International benchmark on 1D nonlinear site-response analysis—Validation phase exercise. Bulletin of the Seismological Society of America, 108(2), 876-900. https://doi.org/10.1785/0120170210.

Riga E., Makra K. & Pitilakis K. (2016) - Aggravation factors for seismic response of sedimentary basins: A code-oriented parametric study. Soil Dyn. Earthq. Eng., 91, 116-132

Riepl J., Bard P.Y., Hatzfeld D., Papaioannou C. & Nechtschein S. (1998) - Detailed evaluation of site-response estimation methods across and along the sedimentary valley of Volvi (EURO-SEISTEST). Bulletin of the Seismological Society of America, 88(2), 488-502.

Rodriguez-Marek A., Cotton F., Abrahamson N.A., Akkar S., Al Atik L., Edwards B., Gonzalo A. Montalva & Dawood, H. M. (2013). A model for single-station standard deviation using data from various tectonic regions. Bulletin of the Seismological Society of America, 103(6), 3149-3163. https://doi.org/10.1785/0120130030.

Rodriguez-Marek A., Montalva G.A., Cotton F. & Bonilla F. (2011) - Analysis of single-station standard deviation using the KiK-net data. Bulletin of the Seismological Society of America, 101(3), 1242-1258, https://doi.org/10.1785/0120100252.

Rodriguez-Marek A., Rathje E.M., Bommer J.J., Scherbaum F. & Stafford P.J. (2014) - Application of single-station sigma and site-response characterization in a probabilistic seismic-hazard analysis for a new nuclear site. Bulletin of the Seismological Society of America, 104(4), 1601-1619. https://doi.org/10.1785/0120130196.

Sánchez-Sesma F., Chávez-Pérez S., Suarez M., Bravo M.A. & Pérez-Rocha L.E. (1988) - The Mexico earthquake of September 19, 1985 - On the seismic response of the Valley of Mexico. Earthquake spectra, 4(3), 569-589.

Schnabel P., Seed H.B. & Lysmer J. (1972) - Modification of seismograph records for effect of local soil conditions, Bull. Seism. Soc. Am. 62, 1649-1664.

Seyhan E. & Stewart J.P. (2014) - Semi-empirical nonlinear site amplification from NGA-West 2 data and simulations. Earthquake Spectra, 30, 1241-1256.

Stewart J.P., Douglas J., Javanbarg M., Bozorgnia Y., Abrahamson N.A., Boore D.M., Campbell K.W., Delavaud E., Erdik M. & Stafford P. J. (2015) - Selection of ground motion prediction equations for the global earthquake model. Earthquake Spectra, 31(1), 19-45.

Stewart J.P., Goulet C., Bazzurro P. & Claasse R. (2006) - Implementation of 1D ground response analysis in probabilistic assessments of ground shaking potential. Presented in GeoCongress 2006, Feb. 26 – March 6p.

Stewart J.P., On-Lei Kwok A., Hashash Y.M.A., Matasovic N., Pyke R., Wang Z., Yang Z. (2008) - Benchmarking of Nonlinear Geotechnical Ground Response Analysis Procedures, Pacific Earthquake Engineering Research Center. University of California, Berkeley. https://peer.berkeley.edu/sites/default/files/web_peer804_onathan_p._stewart_annie_on-lei_kwok.pdf

Toro G.R., Abrahamson N.A. & Schneider J.F. (1997) - Model of strong ground-motions from earthquakes in central and eastern North America: best estimates and uncertainties. Seismological Research Letters, 68(1), 41-57.

Van Houtte C., Drouet S., & Cotton F. (2011) - Analysis of the origins of κ (kappa) to compute hard rock to rock adjustment factors for GMPEs. Bulletin of the Seismological Society of America, 101(6), 2926-2941.

Weatherill, G., Kotha, S. R., & Cotton, F. (2020) - A regionally-adapTable "scaled backbone" ground motion logic tree for shallow seismicity in Europe: Application to the 2020 European seismic hazard model. Bulletin of Earthquake Engineering, 18(11), 5087-5117.

Woessner J., Laurentiu D., Giardini D., Crowley H., Cotton F., Grünthal G., Valensise G., Arvidsson R., Basili R., Demircioglu M.B., Hiemer S., Meletti C., Musson R.W., Rovida A.N., Sesetyan K., Stucchi M. & The SHARE Consortium (2015) - The 2013 European seismic hazard model: key components and results. Bulletin of Earthquake Engineering, 13(12), 3553-3596, https://doi.org/10.1007/s10518-015-9795-1.

Zhao J.X., Zhang J., Asano A., Ohno Y., Oouchi T., Takahashi T., Ogawa H., Irikura K., Thio H.K., Somerville P.G., Fukushima Y. & Fukushima Y. (2006) - Attenuation relations of strong ground motion in Japan using site classification based on predominant period. Bulletin of the Seismological Society of America, 96(3), 898-913. https://doi.org/10.1785/0120050122.